


Mercury cycling and isotopic fractionation in global forests

Xun Wang, Wei Yuan, Che-Jen Lin & Xinbin Feng


To cite this article: Xun Wang, Wei Yuan, Che-Jen Lin & Xinbin Feng (2021): Mercury cycling and isotopic fractionation in global forests, *Critical Reviews in Environmental Science and Technology*, DOI: [10.1080/10643389.2021.1961505](https://doi.org/10.1080/10643389.2021.1961505)

To link to this article: <https://doi.org/10.1080/10643389.2021.1961505>

 View supplementary material 

 Published online: 12 Aug 2021.

 Submit your article to this journal 

 Article views: 380

 View related articles 

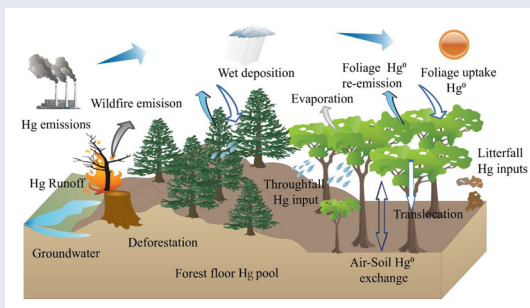
Mercury cycling and isotopic fractionation in global forests

Xun Wang^a, Wei Yuan^a, Che-Jen Lin^{b,c}, and Xinbin Feng^{a,d} 

^aState Key Laboratory of Environmental Geochemistry, Institute of Geochemistry, Chinese Academy of Sciences, Guiyang, China; ^bCenter for Advances in Water and Air Quality, Lamar University, Beaumont, TX, USA; ^cDepartment of Civil and Environmental Engineering, Lamar University, Beaumont, TX, USA; ^dCenter for Excellence in Quaternary Science and Global Change, Chinese Academy of Sciences, Xian, China

ABSTRACT

Forest ecosystem accounts for 31% of global land areas and plays a key role in the global biogeochemical cycling of mercury (Hg). In this critical review, datasets of Hg flux measurements and Hg isotopic compositions in the environmental compartments of forests in the last three decades are synthesized to examine the budgets of Hg mass balance and storages. The primary goal of this synthesis is to provide insight into the source, transportation, translocation and fate of legacy Hg in forests. Existing data indicate that forests represent the largest atmospheric Hg sink in the terrestrial ecosystem, with atmospheric total Hg deposition of 2200–3400 Mg yr⁻¹ (i.e., relative to 40–65% atmospheric Hg pool size) and 500–1100 Gg of Hg stored in surface soils and vegetation. The climate and land cover changes, deforestation and wildfire re-volatilize several hundred tons of Hg into the atmosphere, thus increasing the ecological risk to the regional and global environments. Vegetative uptake of Hg⁰ vapor from air predominantly controls Hg accumulation and isotopic fractionation in the atmosphere and in global forests. With the ongoing Hg emission reduction from anthropogenic sources required by the Minamata Convention, an integrated assessment on the changing biogeochemical processes and isotopic fractionation in response to human and natural perturbations of emissions, climate, and land use is needed.





Existing data indicate that forests represent the largest atmospheric Hg sink in the terrestrial ecosystem, with atmospheric total Hg deposition of 2200–3400 Mg yr⁻¹ (i.e., relative to 40–65% atmospheric Hg pool size) and 500–1100 Gg of Hg stored in surface soils and vegetation. The climate and land cover changes, deforestation and wildfire re-volatilize several hundred tons of Hg into the atmosphere, thus increasing the ecological risk to the regional and global environments. Vegetative uptake of Hg⁰ vapor from air predominantly controls Hg accumulation and isotopic fractionation in the atmosphere and in global forests. With the ongoing Hg emission reduction from anthropogenic sources required by the Minamata Convention, an integrated assessment on the changing biogeochemical processes and isotopic fractionation in response to human and natural perturbations of emissions, climate, and land use is needed.


KEYWORDS Climate change; forest ecosystems; mercury biogeochemical cycling; mercury isotopes

HANDLING EDITORS Jörg Rinklebe and Lena Ma

1. Introduction

Mercury (Hg) in the environment is of broad public health concern because it is persistent, highly mobile through air transport, and its neurotoxic form, methylmercury (MeHg), bioaccumulates in organisms and biomagnifies in food chains (UN-Environment, 2019). The cumulative anthropogenic Hg emissions into the atmosphere have been estimated to be up to 210 Gg since the year of 1850 (Streets et al., 2011), which causes global Hg pollution nearby the sources and in remote regions via long-range transport, and draws concerns on health of wildlife and humans. To protect public health and the environment from impacts of anthropogenic Hg emissions, Minamata Convention on Mercury, a legally binding international treaty, entered into force in August 2017.

CONTACT Xinbin Feng  fengxinbin@vip.skleg.cn  State Key Laboratory of Environmental Geochemistry, Institute of Geochemistry, Chinese Academy of Sciences, Guiyang, China.

 Supplemental data for this article can be accessed at [publisher's website](#).

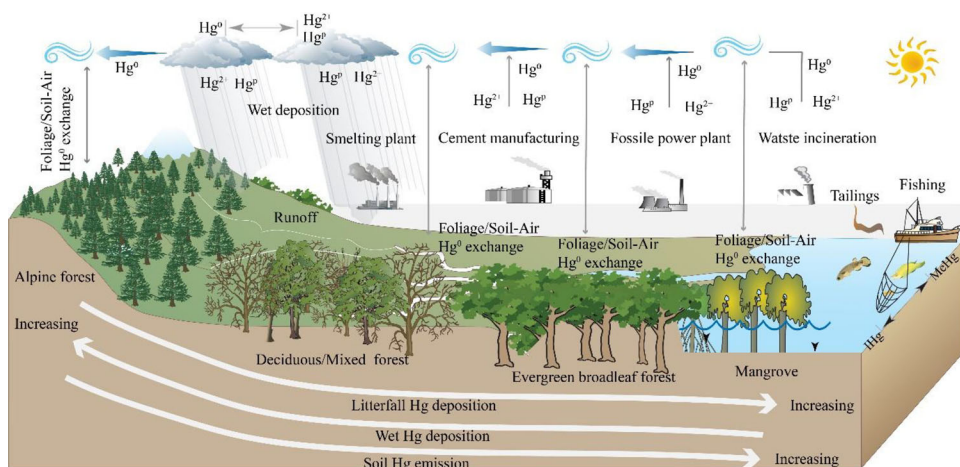


Figure 1. Mercury transport from the anthropogenic sources to the forest ecosystems. The litterfall Hg deposition and soil Hg emissions typically decrease from low elevation/latitude evergreen broadleaf forest to the alpine/boreal forest, while the wet deposition shows an increasing trend.

Anthropogenic release of Hg into the atmosphere consists of three species: gaseous oxidized Hg (Hg^{2+}), particle-bound Hg (Hg^{P}) and gaseous elemental Hg (Hg^0). Given their active physical and chemical properties, Hg^{2+} and Hg^{P} can be quickly scavenged from the atmosphere via wet and dry depositions onto the Earth's surface (Lindberg et al., 2007; Selin, 2009). In contrast, gaseous Hg^0 has a long residence time (0.5–1 year) in the atmosphere due to its relatively inert reactivity (Lindberg et al., 2007). Hg^0 can also be removed from air after slowly oxidized to Hg^{2+} or Hg^{P} through complex reactions mediated by oxidants such as O_3 , $\bullet\text{OH}$ and Br in the air (Lindberg et al., 2007; Mao et al., 2016; Wang et al., 2018). In the terrestrial ecosystems, another scavenging process of Hg^0 is through vegetation uptake followed by litterfall deposition into the forest floor (Jiskra et al., 2018; Wang et al., 2019c; Zhou et al., 2021). Forest ecosystem accounts for 31% of global land areas and is a hotspot region for the global biogeochemical cycling of Hg (Grigal, 2003; Wang et al., 2017b). A substantial quantity of anthropogenic Hg is accumulated and stored in forested areas through uptake, litterfall, throughfall and translocation to woods (Fig. 1). Forest represents the important global Hg pool, which shapes the Hg accumulation in terrestrial biota (Lindberg et al., 2007), re-emissions back to atmosphere (Gabriel et al., 2005), and transport to downstream aquatic ecosystems where methyl Hg is produced, bioaccumulated and biomagnified (Feng et al., 2010). Understanding Hg cycling in forests is critical in assessing the effectiveness of emission reduction in anthropogenic sources mandated by the Minamata Convention.

The recognition of the importance of the role that global forests play in Hg cycling began in the 1990s, when studies in Northern Europe found that litterfall and throughfall Hg deposition in forests exceeded direct open-field wet deposition by severalfold (Gustin, et al. 1999; Lee et al., 1998; Lindberg et al., 1995; Meili, 1991a, 1991b). From 1990s to 2010s, extensive measurements of Hg fluxes in forest ecosystems worldwide were reported, attempting to quantify the mass budget of Hg in forest. Since 2010s, advanced analytical techniques of Hg stable isotopes were applied to trace the source, transportation, accumulation, and storage of Hg caused by the biogeochemical processes taking place in the air-vegetation-water-soil ecosystem.

This critical review synthesizes and illustrates the biogeochemical cycling of Hg in remote forests (far away from urban regions and without distinct Hg emission sources nearby) as well as the resulted isotopic fractionation based on the literature published in the last three decades. We comprehensively collected Hg concentrations (~2400 records), fluxes (~200 sites) and isotopic composition (~1700 records) data from more than 250 peer-reviewed publications. Using the compiled datasets, four biogeochemical processes with values of forced isotopic fractionation in forests are

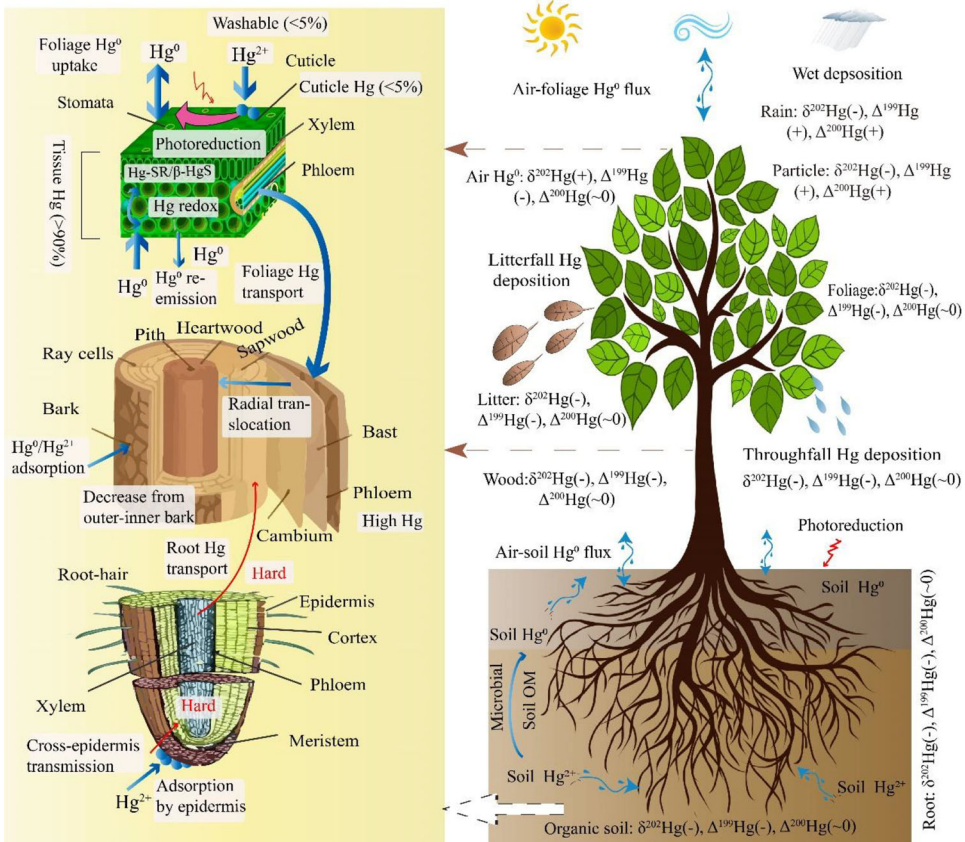


Figure 2. Left panel: mechanism of tree uptake atmospheric mercury (Hg) through their foliage via stomatal and cuticular uptake, and transporting Hg through leaf tissues and translocating Hg via phloem transport to woody tissues. Tree also takes up Hg from the soil through their roots, with little transport of Hg through root tissues into xylem. Right panel: Hg biogeochemical processes and the Hg stable isotopic compositions in forests.

presented (Fig. 2). The first process is Hg exchange over the interface of the air-foliage surface, i.e., atmospheric Hg^0 uptake or re-emission through the stomata of foliage, and atmospheric Hg^{2+} or Hg^p absorption by the cuticle and then the photo-reduction induced Hg^0 re-emission. The second is Hg exchange between plant-soil, which includes root uptake the Hg^{2+} from the soil solution and little Hg transport to the xylem driven by the transpiration, and litterfall Hg deposition into the forest floor. The third is Hg exchange between the surface of soil and air, including the atmospheric Hg^0 direct deposition and oxidation in soils, and reduction induced Hg^0 re-emission from the soil surface (photo-reduction, microbial reduction and organic matter reduction). The fourth is the Hg transport budget associated with hydrological processes such as rainfall, throughfall and runoff. In this synthesis, the transformation and accumulation of MeHg in forests are not included since the conversion of inorganic Hg to MeHg is not prevalent (e.g., the ratio of MeHg/THg in forest soils <1%) in forest ecosystems (Grigal, 2003; Selvendiran et al., 2008b; St Louis et al., 2001).

2. Hg distribution across the global forests

2.1. Hg distributions in vegetation

The concentration of Hg in vegetation biomass across the globe ranks as follows (Figs. 3A, 3B, and S1): litterfall (median = 40.0 ng g^{-1} , mean = $49.5 \pm 31.5 \text{ ng g}^{-1}$, in 317 tree species) > foliage

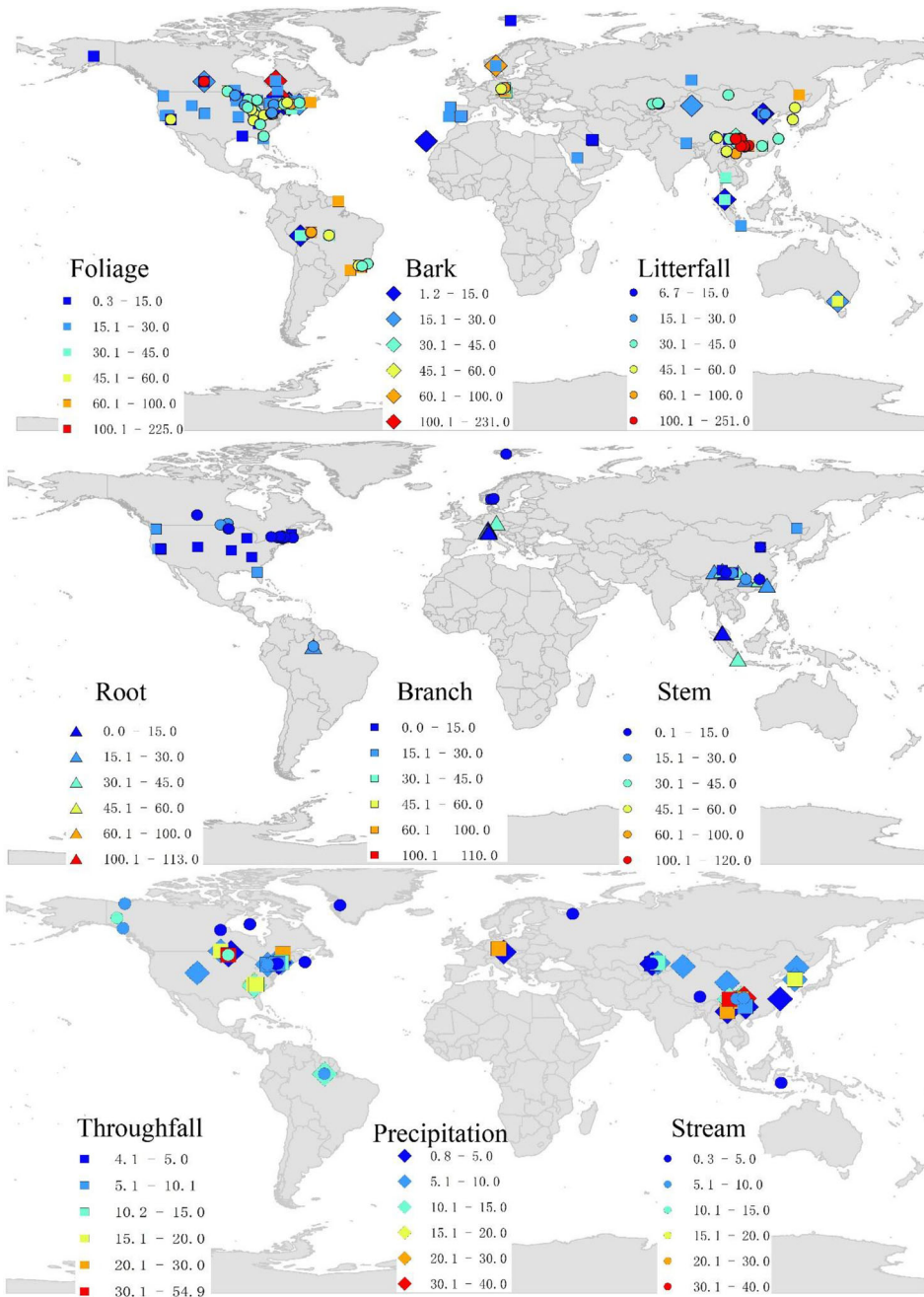


Figure 3. Hg concentration in forest ecosystems across the globe from the database presented in this work. The unit for the vegetation Hg concentration is ng g^{-1} , and for the water samples is ng L^{-1} .

(median = 28.7 ng g^{-1} , mean = $35.4 \pm 30.0 \text{ ng g}^{-1}$, in 412 tree species) > root (median = 14.5 ng g^{-1} , mean = $22.5 \pm 22.9 \text{ ng g}^{-1}$, in 61 tree species) or bark (median = 14.7 ng g^{-1} , mean = $27.9 \pm 45.6 \text{ ng g}^{-1}$, in 65 tree species) > branch/twig (median = 13.1 ng g^{-1} , mean = $17.0 \pm 11.6 \text{ ng g}^{-1}$, in 41 tree species) > stem (median = 2.8 ng g^{-1} , mean = $6.0 \pm 7.0 \text{ ng g}^{-1}$, in 115 tree species). This descending order of Hg concentration in plants is different from those

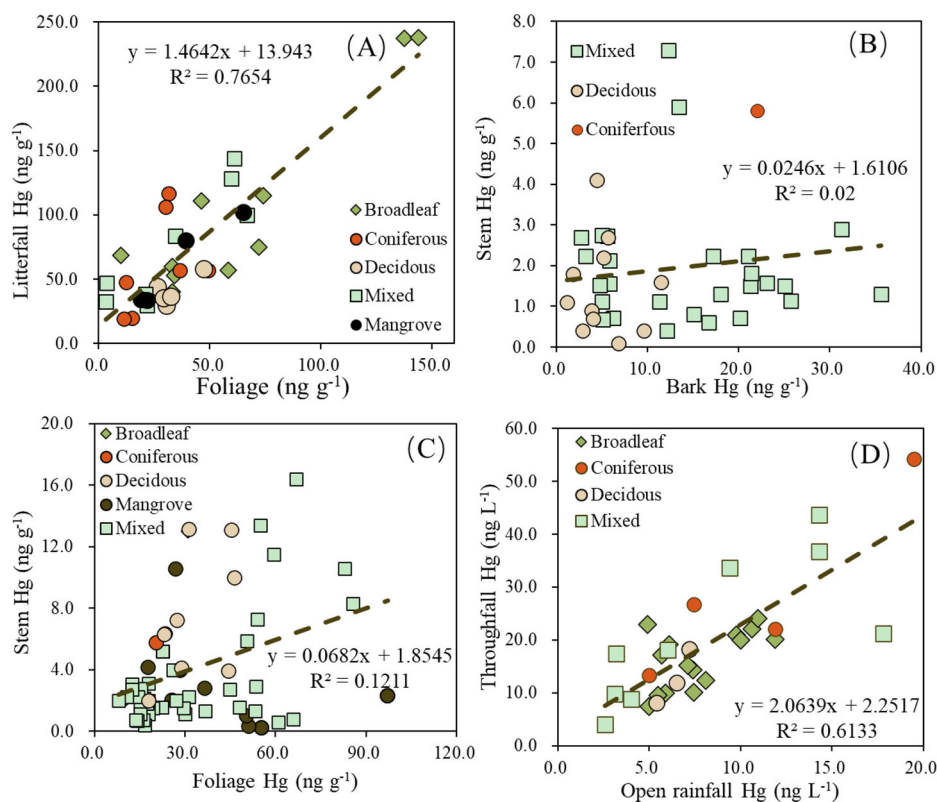


Figure 4. Correlations (A) between the foliage Hg and litterfall Hg, (B) between the stem Hg and bark Hg, (C) between the foliage Hg and stem Hg, (D) between the open rainfall Hg and the throughfall Hg in the database compiled here.

found for other heavy metals (e.g., Pb, Cd, etc.), which typically show highest concentrations in roots (Rodríguez Martín et al., 2018; Tang et al., 2015; Zayed et al., 1992). This is because heavy metals are mainly bounded to the air particle, while more than 95% Hg in air exists as the Hg⁰ vapor (Lindberg et al., 2007; Obrist et al., 2018). Therefore, Hg can be readily incorporated into the biomass through foliage uptake of atmospheric Hg⁰, but the other metals are mainly derived from root uptake.

Forest type is an important factor that influences the Hg distribution (Fig. S2). The mangrove and evergreen broadleaf tree species have a higher Hg concentration in foliage and litterfall ($P < .05$ by Kruskal-Wallis test). The median value of foliage Hg is 56.0 ng g⁻¹, 33.6 ng g⁻¹, 27.6 ng g⁻¹ and 23.0 ng g⁻¹ for broadleaf, mangrove, coniferous and deciduous tree species, while the median value of litterfall is 57.0 ng g⁻¹, 80.0 ng g⁻¹, 35.0 ng g⁻¹ and 36.5 ng g⁻¹, respectively. Across the global forests, the regions at lower altitudes have higher foliage Hg concentrations due to the predominant distribution of broadleaf and mangrove forests (Fig. 3A). Hg concentrations in bark, stem and root show large variations and are site-specific. The median value of bark for broadleaf, mangrove, coniferous and deciduous tree species is 7.0 ng g⁻¹, 1.6 ng g⁻¹, 25.7 ng g⁻¹ and 11.3 ng g⁻¹, and stem Hg is 9.3 ng g⁻¹, 2.8 ng g⁻¹, 2.7 ng g⁻¹ and 2.1 ng g⁻¹, and root Hg is 25.0 ng g⁻¹, 17.6 ng g⁻¹, 7.0 ng g⁻¹ and 13.3 ng g⁻¹, respectively. In addition, the foliage Hg shows a positive correlation to the litterfall Hg ($P < .05$, $R^2 = 0.77$) and to the stem Hg ($P < .05$, $R^2 = 0.12$; Fig. 4A and 4C). However, there is no significant correlations between stem Hg with bark Hg or with the root Hg ($P > .05$, Fig. 4B). These observations point to the translocation of Hg in vegetation after atmospheric Hg⁰ uptake by foliage.

2.2. Mechanism of Hg uptake and translocation in vegetation

Two potential pathways for the foliage uptake of atmospheric Hg have been proposed (Fig. 2). One is through stomatal uptake of atmospheric Hg^0 . Extensive field data have shown that higher deposition to the foliage occurs at elevated air Hg^0 , and that foliage Hg accumulation rate is closely correlated with stomatal density (Demers et al., 2013a; Ericksen et al., 2003; Frescholtz et al., 2003; Hanson et al., 1995; Laacouri et al., 2013; Stamenkovic & Gustin, 2009). The other is the nonstomatal uptake, which is suggested dominant at night and atmospheric Hg deposited to the surface of foliage, then incorporated into the leaf tissue and not released back into the air (Arnold et al., 2018; Stamenkovic & Gustin, 2009). Foliage cuticles contain both polar and nonpolar routes, and allow both Hg^0 (nonpolar) and Hg^{2+} (polar) to pass through the cuticle. Therefore, it is likely that cuticles involve in the nonstomatal route (Arnold et al., 2018; Laacouri et al., 2013; Stamenkovic & Gustin, 2009). Field observations also indicated that the night nonstomatal route could lead to a depletion of atmospheric Hg^0 under calm, stable boundary layers in forests (Fu et al., 2016).

Scanning electron microscopy and radioactive assays show that deposition Hg^0 through uptake is bound to the epidermal and stomatal cell walls or adsorbed to leaf surface (Amado Filho et al., 2002). Laacouri et al. (2013) reported >90% Hg is stored in the foliage tissue and 2–6% in cuticle or the surface of foliage for the common deciduous tree species, suggesting stomatal uptake of atmospheric Hg as the potential pathway (Fig. 2). Yuan et al. (2019a) estimated that 30% of acquired Hg can re-emit back to air after not-yet-identified Hg^{2+} reduction in foliage tissues. With the high energy resolution X-ray absorption near-edge structure (HR-XANES) spectroscopy, up to 57% of stored Hg species in foliage exists as nanoparticles, with the remainder speciated as a bis-thiolate complex (i.e., $\text{Hg}(\text{SR})_2$) (Manceau et al., 2018). The formation of Hg nanoparticles in foliage is controlled by the process of nucleation and growth from Hg complexes (Manceau et al., 2015). This explains the increasing Hg concentration during leaf senescence since the nutrient translocation before the leaf abscission and immobile of Hg which significantly decrease the mass density and increase Hg concentration in litterfall.

The spatial distribution of foliage Hg in global forests is largely influenced by the variation in atmospheric Hg^0 and in tree physiological processes (Wang et al., 2017a, 2020a). Potted plant experiments in the laboratory have demonstrated linear correlation between foliage Hg and air Hg concentration (Arnold et al., 2018; Ericksen et al., 2003; Frescholtz et al., 2003; Leonard et al., 1998a, 1998b; Stamenkovic et al., 2008), although changes of air Hg^0 concentration cannot solely explain the foliage Hg accumulation in field observations. For example, the remote and rural regions in China typically have higher total atmospheric Hg concentration (usually $1\text{--}5\text{ ng m}^{-3}$) than in North America ($1\text{--}2\text{ ng m}^{-3}$) while the foliage Hg concentration for same type of forest in China shows insignificant difference to the concentration in North America (Figs. S3 and S4). The observational discrepancies reflect the active response of foliage to the atmospheric Hg^0 under different climates and tree physiological parameters such as rate of net photosynthesis, stomata conductance, transpiration rate and leaf lifespan, etc. Plant physiology also explains the higher Hg concentration in evergreen broadleaf and mangrove tree species than those found in deciduous and coniferous tree species. The longer foliage lifespan of evergreen broadleaf species (~ 1 year compared to several months of deciduous species) and greater stomata conductance facilitate an extended and stronger atmospheric Hg^0 exchange (Hanson et al., 1995; Poissant et al., 2008; Yuan et al., 2019a).

The translocation of Hg in vegetation was hypothesized to be similar to most heavy metals that initiate from root uptake of Hg^{2+} in soil solution, followed by root to foliage transport via plant xylem sap during the evapotranspiration process (Bishop et al., 1998; Godbold & Huttermann, 1985; Lindberg et al., 2002). However, experimental and field measurements suggest that up to 90% Hg in the root zone is bound to the cell walls and membranes of fine roots in the uptake process (Cui et al., 2014; Wang et al., 2012), and only a small amount of Hg in roots

(<5%) can be translocated to the aboveground woody biomass, and nearly no root derived Hg can re-emit to the air (Arnold et al., 2018; Graydon et al., 2009; Greger et al., 2005). An observed exception is that the root of wetland grass has a greater ability to take up soil Hg and transport to the aboveground parts (Meng et al., 2018). Recent observations using stable Hg isotope techniques (spike and natural stable isotopic compositions) support the translocation of Hg from foliage to stem via the phloem as the main pathway for Hg accumulation in aboveground woods (Graydon et al., 2009; Wang et al., 2020b, 2021b). Due to the loose porous structure, bark has a strong absorption of atmospheric Hg, particularly for particle-bounded Hg, and therefore exhibit a higher Hg concentration compared to those found in wood (Hanson et al., 1997; Rodríguez Martín et al., 2018). However, the lack of correlation between bark and stem likely suggests the little Hg surpass bark to wood and vice versa (Fig. 4B). The Hg concentration decreases from the outer to the inner bark, yet elevated Hg in phloem (Novakova et al., 2021). This confirms the importance of phloem Hg translocation from foliage. Studies of Hg distribution in tree-ring have reported the radial Hg translocation from the sapwood to the heartwood (Arnold et al., 2018; Chellman et al., 2020; Novakova et al., 2021; Schneider et al., 2019; Wang et al., 2021b). The radial translocation in woody biomass depends on the tree species and tree-age related sapwood rings. The tree species with relatively low and consistent number of sapwood tree rings typically exhibit a weaker radial translocation (Chellman et al., 2020; Novakova et al., 2021; Wang et al., 2021b).

Tree woody biomass is not a passive bio-monitor. The observed variations of Hg concentration in wood are a result of complex physiological interactions between the vegetation and the environment. These causes for the variabilities of Hg concentration in woody biomass among different forest types are not well understood, but two explanations have been hypothesized to explain the observed difference. One is tree physiological factors that influence foliage Hg uptake from the atmosphere and Hg translocation in phloem and xylem. These factors include but are not limited to the asymmetrical growth of trees, stomata conductance, tree ages and canopy dynamics. Another explanation is the environmental factors such as soil moisture, hill slope, wind direction, soil nutrients, air temperature and precipitation, which indirectly influence the tree physiology that controls Hg accumulation in wood (Clackett et al., 2018; Ghotra et al., 2020; Scanlon et al., 2020; Wang et al., 2021b).

2.3. Hg transport through the hydrological processes in forests

Hg concentrations and variations in rainfall, throughfall and stream/runoff have been relatively well documented. The median value of Hg concentration in open-field rainfall is 7.4 ng L^{-1} (mean = $7.8 \pm 5.5 \text{ ng L}^{-1}$, $n = 69$ sites), in throughfall is 20.1 ng L^{-1} (mean = $23.7 \pm 15.8 \text{ ng L}^{-1}$, $n = 54$ sites), and in forest stream/runoff is 5.0 ng L^{-1} (mean = $6.4 \pm 6.0 \text{ ng L}^{-1}$, $n = 106$ sites) in Fig. 3(C). The open-field rainfall Hg concentration shows significant positive correlation to the throughfall Hg ($R^2 = 0.61$, $P < .05$), with a slope of 2.0 for throughfall Hg to the rainfall Hg at paired sites across the globe (Fig. 4D). The median rainfall Hg in broadleaf, coniferous, deciduous and mixed forests is 9.2 ng L^{-1} , 6.1 ng L^{-1} , 6.5 ng L^{-1} , and 7.1 ng L^{-1} , for throughfall Hg is 22.5 ng L^{-1} , 18.2 ng L^{-1} , 11.0 ng L^{-1} , and 18.2 ng L^{-1} , for stream/runoff Hg is 4.8 ng L^{-1} , 4.3 ng L^{-1} , 4.4 ng L^{-1} , and 5.3 ng L^{-1} , respectively (Fig. S5). The Hg concentrations in these water samples do not differ significantly, except the higher Hg concentrations observed in evergreen broadleaf forests. It is noteworthy that the datasets for broadleaf rainfall Hg concentration were mainly collected in China and Brazil with greater anthropogenic Hg emissions. Therefore, the elevated rainfall Hg likely reflects the regionally higher atmospheric Hg pollution level (Streets et al., 2005, 2011; Wu et al., 2016).

The canopy structure and characteristics play an important role in modifying the Hg concentration in throughfall. Field observations have suggested that elevated Hg in throughfall is closely

related to the pathway of rainfall scavenging deposited Hg^{2+} and Hg^{P} on canopy surface (Graydon et al., 2008; Hultberg et al., 1995; Rea et al., 1996, 2001; St Louis et al., 2001). A recent study with the Hg isotopes has demonstrated that Hg can also be derived from the canopy epiphyte cover and tree detritus which formed by the degraded vegetation biomasses (Wang et al., 2020b). For stream/runoff Hg, the low Hg concentrations have been attributed to soil interception of particle-bounded Hg and selective absorption of dissolved Hg by organic matters when the water leaches through soil (Allan et al., 2001; Eklof et al., 2013; Lee et al., 2000; Lin et al., 2011; Schwesig & Matzner, 2000; Zhao et al., 2015). The source of stream/runoff Hg during the process of Hg desorbed from soil or decomposing litter derived from isotopic evidence (Jiskra et al., 2017; Tsui et al., 2020; Woerndle et al., 2018) is discussed in Sec. 4.

The Hg variation in other hydrological processes has been not well documented. Several studies reported Hg concentration in leaching soil water and groundwater is typically lower than 10 ng L^{-1} (Selvendiran et al., 2008a; Sun et al., 2019b; Vidon et al., 2013). The land covers, hydrogeomorphic setting of the forest zone (e.g., topography, soil type, layer depth), and groundwater chemistry especially the DOC (dissolved organic carbon) concentration and quality control the Hg variations (Selvendiran et al., 2008a; Sun et al., 2019b; Vidon et al., 2013). Relatively few studies have documented Hg concentrations in transpiration and evaporation water, and Hg concentrations in xylem sap. Bishop et al. (1998) reported concentrations of Hg in xylem sap ranged from $10\text{--}15 \text{ ng L}^{-1}$ in both the Scots pine and Norway spruce, and of MeHg at $0.03\text{--}0.16 \text{ ng L}^{-1}$. The Hg concentration in xylem sap of sugar maple is reported in the range of $1.6\text{--}10.4 \text{ ng L}^{-1}$, but shows insignificant correlation to the soil Hg concentration (Yanai et al., 2020). Further studies are needed to understand whether the process of plant and soil transpiration and evaporation leads to a significant Hg emission.

2.4. Hg accumulation in soils

The process of litter decomposition influences the fate of Hg stored in litter and the subsequent accumulation in soils and re-emission of Hg. Since Hg in litter and soil is strongly bound to organic matters, earlier studies have quantified the change of Hg concentration and its stoichiometry with carbon, nitrogen, and sulfur in soil profiles. The observed Hg/C ratio increases with decreasing C/N ratio in soils, leading to high levels of Hg in the decomposed litter (Gong et al., 2014; Obrist et al., 2011; Wang et al., 2016b). Hg is efficiently retained in organic matter while C is lost during mineralization and the additional Hg uptake by decomposing litter also occur due to the selective Hg sorption to different organic matter fractions (Demers et al., 2013b; Gong et al., 2014; Obrist et al., 2011; Wang et al., 2016b).

Controlled laboratory litter incubation studies found a significant loss of Hg^0 when disconnected from the atmospheric Hg inputs (Pokharel & Obrist, 2011). Field litter decomposition experiments in boreal and alpine forests in 1–2 years of experimental period have verified the significant Hg mass increase during decomposition (Demers et al., 2007; Pokharel & Obrist, 2011; Wang et al., 2016b, 2019d). These additional Hg sources are attributed to: (1) the wet and dry deposition of Hg^{2+} and Hg^{P} , particularly the throughfall Hg inputs, (2) the microbial immobilization of Hg^0 or the functional group oxidation of Hg^0 in the surface of decomposing litter, and (3) fungal translocation of old Hg from lower soils to the decomposing litter (Demers et al., 2007; Wang et al., 2016b, 2019d). Both litter type and climate factors influence Hg transformation during litter decomposition (Pokharel & Obrist, 2011; Wang et al., 2016b, 2019d). Increase in temperature by $1\text{--}2 \text{ }^\circ\text{C}$ promotes Hg mass increments during decomposition at Mt. Ailao (Wang et al., 2016b). The litter decomposition rate is another parameter to control the Hg accumulation. A faster litter decomposition rate decreases the Hg mass in the decomposing litter (Wang et al., 2019d), as evidenced by the experiments in subtropical evergreen forest observing greater Hg mass loss due to the higher nutrient turn rates (Wang et al., 2019d,

2021a). However, few studies have depicted Hg variations during litter decomposition in the tropical rainfall forests where with the elevated temperature, precipitation and nutrient cycling rates. The lack of knowledge of tropical forests largely constrains our understanding of Hg accumulation in global forests.

Across the globe, the soil Hg concentration in remote forests varies largely (several tens to hundreds ng g^{-1}) due to the complicated impacts from the vegetation, climate and topographic factors (Obrist et al., 2016; Outridge et al., 2018; Wang et al., 2019c). Wang et al. (2019c) estimated the global surface soil Hg spatial distribution and suggested the climate and vegetation as the primary drivers. Generally, the surface soil Hg concentration (e.g., 0–20 cm) among different forests is the result of vegetation induced atmospheric Hg inputs and the Hg variations during litter mineralization caused by the accumulation and uptake of organic matter, and the Hg loss via the re-emission and runoff, and Hg mixing from various Hg sources (Grigal, 2003; Wang et al., 2019c). At specific forest site, the Hg concentration usually shows an increase gradient from Oi (litters), Oe (decomposed litters) to Oa (well decomposed humus soil), and then a decrease trend from mineral soil to soil parent materials. The increasing gradient in soil profiles mainly reflects the Hg enhanced accumulation or additional Hg uptake from environment during the litter decomposition, and the decreasing trend mainly represents the low Hg mixing from the deep soils and the Hg loss during the long-term soil development (Lu et al., 2021; Luo et al., 2014; Navratil et al., 2014; Obrist et al., 2011; Wang et al., 2019c).

3. Hg mass balance and Pool size in forests

3.1. Hg flux measurement in forests

The median value for open-field precipitation flux reported in the literature is $8.8 \mu\text{g m}^{-2}\text{yr}^{-1}$ (mean = $9.3 \pm 4.3 \mu\text{g m}^{-2}\text{yr}^{-1}$, $n=98$ sites), for throughfall Hg deposition is $14.0 \mu\text{g m}^{-2}\text{yr}^{-1}$ (mean = $18.5 \pm 15.5 \mu\text{g m}^{-2}\text{yr}^{-1}$, $n=64$ sites), for litterfall Hg deposition is $15.3 \mu\text{g m}^{-2}\text{yr}^{-1}$ (mean = $26.4 \pm 30.5 \mu\text{g m}^{-2}\text{yr}^{-1}$, $n=161$ sites), and for runoff flux is $2.5 \mu\text{g m}^{-2}\text{yr}^{-1}$ (mean = $4.6 \pm 5.5 \mu\text{g m}^{-2}\text{yr}^{-1}$, $n=29$ sites) and for soil Hg emission is $14.0 \mu\text{g m}^{-2}\text{yr}^{-1}$ (mean = $22.2 \pm 24.8 \mu\text{g m}^{-2}\text{yr}^{-1}$, $n=21$ sites). The rainfall Hg concentration and deposition do not show significant difference among coniferous, deciduous and mixed forests. Precipitation and Hg concentration in broadleaf forests are generally greater, leading to 50% to 60% higher Hg deposition compared to those observed in other forest types (Fig. 5). In addition, the litterfall Hg deposition in the broadleaf forest has the highest value due to the elevated litter Hg concentration and biomass production. The deciduous forest has the lowest throughfall Hg and litterfall Hg depositions due to its thinner forest canopy (Fig. 5).

Globally, the spatial variation of rainfall Hg deposition is predominantly controlled by precipitation, which shows a higher correlation to rainfall Hg deposition than rainfall Hg concentration ($R^2=0.45$ vs. $R^2=0.29$). Similarly, the litterfall biomass production contributes more significantly than the litterfall Hg concentration for the observed spatial change of litterfall Hg deposition ($R^2=0.61$ vs. $R^2=0.20$). In contrast, throughfall Hg concentration has a higher contribution to the variation of throughfall Hg deposition ($R^2=0.62$ vs. $R^2=0.49$) because the scavenging additional Hg from the canopy increases the Hg concentration in throughfall. Precipitation is positively correlated to throughfall and rainfall Hg depositions, and to litterfall Hg deposition due to the increased canopy biomass production caused by rainfall (Fig. 6A and 6B). The ratio of litterfall to throughfall Hg deposition is 2 to 3 in broadleaf forests, compared to ~ 1 in other forests, suggesting intensive canopy uptake of atmospheric Hg^0 (Fig. 5).

The quantity of Hg output (air-soil flux and runoff flux) from forests has large uncertainties due to limited available data. The reported air-soil Hg flux ranges from -4.6 to $81.4 \mu\text{g m}^{-2}\text{yr}^{-1}$ (a negative value infers air to soil Hg deposition, $n=21$ sites). Air-soil Hg^0 exchange flux is a dynamic bi-directional process, and factors that influence the exchange process include

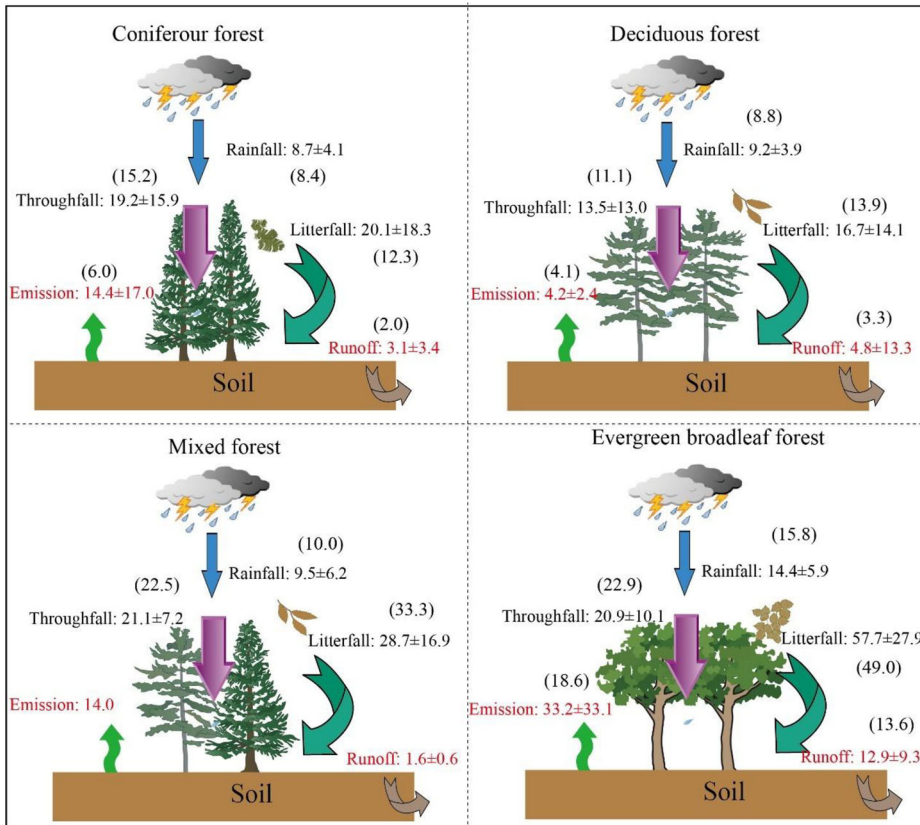


Figure 5. Global Hg mass balance in the forest ecosystems based on the flux database compiled in this work. Notably, the emission flux and runoff flux (in red) have significant uncertainties due to limited data availability. The number in brackets represents the median value.

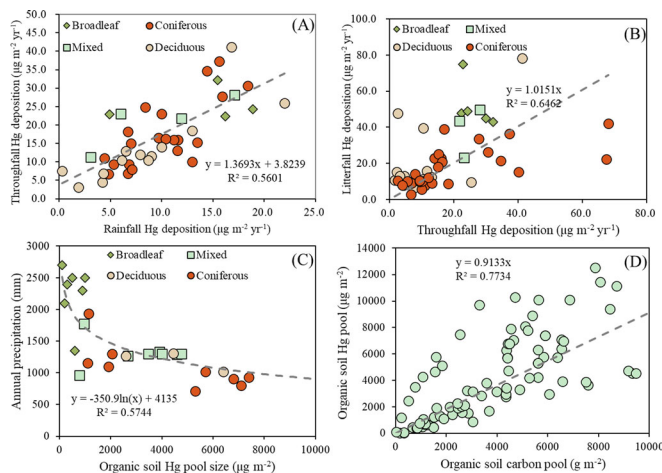


Figure 6. Correlations (A) between the rainfall Hg deposition and the throughfall Hg deposition, (B) between the throughfall Hg deposition and litterfall Hg deposition, (C) between the organic soil Hg pool size and the annual precipitation, (D) between the organic soil carbon pool and organic soil Hg pool in the database compiled in this work.

atmospheric Hg^0 concentration, floor Hg concentrations, soil characteristics, forest types, and climatic factors. Yuan et al. (2019b) summarized the governing climatic factors driving the air-soil Hg^0 exchange flux at global forest sites, and suggested that the dominant factor is temperature

(positive effect, i.e., increases Hg emission), followed by air Hg⁰ concentration (negative effect), humidity (typically positive effect) and solar radiation (positive effect). An increase of temperature accelerates the soil Hg⁰ diffusion and Hg²⁺ reduction in soil profiles (Agnan et al., 2016; Yuan et al., 2019b), thus ongoing global warming likely enhances Hg⁰ evasion from forest floor.

Hg runoff data collected at 29 global forest sites ranges from 1.6 to 21.6 $\mu\text{g m}^{-2}\text{yr}^{-1}$. The evergreen broadleaf forest has a higher runoff Hg flux because of the larger water discharge (Fig. 5). Both hydrological and biogeochemical processes play an important role in the quality of Hg runoff flux (Allan et al., 2001; Bushey et al., 2008; Eklof et al., 2013; Lee et al., 2000; Schwesig & Matzner, 2000). Climate change including incidental extreme weather and wildfires, forest cover types and forestry (i.e., stump harvest) all have impact on Hg runoff flux (Eklof et al., 2012, 2013, 2014; Sorensen et al., 2009).

3.2. Hg mass balance and pool sizes across the globe

The source and sink terms synthesized from published datasets indicate that >60% of atmospheric input Hg (throughfall Hg + litterfall Hg) is retained in the forest ecosystems (Fig. 5), suggesting the forest as an important sink of atmospheric Hg at the global scale. More recently, Yu et al. (2020) reported a lower ratio (5% to 63%) of Hg inputs retained in two subtropical coniferous forests in China based on micrometeorological flux measurement. This difference is likely caused by a combination of the measurement technique and the elevated forest soil Hg concentration that induces high Hg⁰ re-emission.

Though the Hg concentration in wood is one order of magnitude lower than that in foliage, the large biomass of aboveground wood leads to the Hg pool sizes 1 to 2 times greater than the foliage Hg pool sizes (Wang et al., 2020b; Yang et al., 2017). The soil Hg pool size in forests is much larger than the vegetation Hg pool size, with >90% Hg stored in soil (Navratil et al., 2009; Obrist et al., 2009, 2011; Wang et al., 2009, 2020b). From the literature data collected at global forest sites, the organic soil Hg pool size shows a logarithmic decrease with the increasing precipitation intensity (Fig. 6C), reflecting a fast nutrient return that limits Hg accumulation in soil. The organic soil Hg pool size is significantly correlated to the carbon pool size (Fig. 6D), indicating Hg complexation with organic matters and the association of Hg cycle with soil carbon cycle at the continental and global scales (Obrist et al., 2011; Wang et al., 2019c).

We used the median Hg concentrations in rainfall, litterfall and throughfall to estimate the specific deposition as:

$$J_i = C_{\text{Hgi}} \times P_i \quad (1)$$

where i = rainfall, litterfall and throughfall, and J_i is the specific Hg deposition, and C_{Hgi} is the corresponding Hg concentration, and P is the annual of precipitation intensity, or biomass production of litterfall, or throughfall intensity across the globe. The global litterfall Hg deposition is estimated to be in the range of 1000–1200 mg yr^{-1} (Fu et al., 2016; Wang et al., 2016a); wet Hg deposition range is 690–1000 Mg yr^{-1} ; and throughfall Hg deposition range is 1100–1400 Mg yr^{-1} (Fu et al., 2016; Zhou et al., 2021). Wang et al. (2019c) estimated 1088 ± 379 Gg of Hg is stored in 0–20 cm surface soil globally, and 32% of the surface Hg storage resides in tropical/subtropical forest regions, and 23% in temperate/boreal forest regions. Using the median Hg concentration of root and aboveground wood and their biomass (Spawn et al., 2020), the global Hg pool size in underground wood is about 2100 to 3200 Mg, and in aboveground wood is about 1200 to 1950 Mg. The Hg fixed in woody biomass is ~ 140 Mg yr^{-1} (Obrist et al., 2010; Wang et al., 2020b). There are large uncertainties for air-soil Hg flux and runoff, making it difficult to quantify the global budget of forest Hg.

4. Process evidence by stable Hg isotopes in forests

Recent analytical advancements of Hg stable isotopes enable identification of the source, transformation, and fate of Hg in forest ecosystems. Hg undergoes both mass dependent fractionation (MDF, represented by $\delta^{202}\text{Hg}$) and mass independent fractionation (odd-MIF for odd mass number Hg isotopes indicated by $\Delta^{199}\text{Hg}$ or $\Delta^{201}\text{Hg}$; even-MIF represented by $\Delta^{200}\text{Hg}$ or $\Delta^{204}\text{Hg}$) during the processes of transport and transformation. Hg-MDF is reported in δ notation using the unit of permil (‰) referenced to the commonly adopted isotope reference material for Hg, NIST 3133:

$$\delta^{202}\text{Hg}(\text{‰}) = 1000 \times \left[\left(\frac{{}^{202}\text{Hg}/{}^{198}\text{Hg}_{\text{sample}}}{({}^{202}\text{Hg}/{}^{198}\text{Hg}_{\text{NISTSRM3133}})} - 1 \right) \right] \quad (2)$$

Hg-MIF is reported as $\Delta^{\text{xxx}}\text{Hg}$ and calculated using the difference between a measured $\delta^{\text{xxx}}\text{Hg}$ value and a value predicted based on MDF (Blum & Bergquist, 2007):

$$\Delta^{199}\text{Hg}(\text{‰}) = \delta^{199}\text{Hg} - 0.2520 \times \delta^{202}\text{Hg} \quad (3)$$

$$\Delta^{200}\text{Hg}(\text{‰}) = \delta^{200}\text{Hg} - 0.5024 \times \delta^{202}\text{Hg} \quad (4)$$

$$\Delta^{201}\text{Hg}(\text{‰}) = \delta^{201}\text{Hg} - 0.7520 \times \delta^{202}\text{Hg} \quad (5)$$

Earlier works have reviewed the Hg isotopes main processes during the global Hg cycling (Blum et al., 2014; Kwon et al., 2020; Sun et al., 2019a; Tsui et al., 2019). Here we focus on the observed Hg isotopic fractionation in forests and discuss the Hg biogeochemical processes evidenced by stable Hg isotopes.

4.1. Hg isotopic fractionation during air-vegetation exchange processes

Figures 2 and 7 summarize the Hg isotopic compositions of primary endmembers of Hg sources in remote forests. The median value for $\delta^{202}\text{Hg}$ of air Hg^0 globally is 0.27‰ (mean = $0.27 \pm 0.57\text{‰}$, $n = 343$), for $\Delta^{199}\text{Hg}$ is -0.17‰ (mean = $-0.16 \pm 0.11\text{‰}$, $n = 343$), and for $\Delta^{200}\text{Hg}$ is -0.05‰ (mean = $-0.05 \pm 0.05\text{‰}$, $n = 343$). The $\delta^{202}\text{Hg}$ and $\Delta^{199}\text{Hg}$ of the air Hg^0 in China are more positive than in North America and Europe (median of $\delta^{202}\text{Hg}$: 0.12‰ in China vs. 0.55‰ in North America and Europe, and median of $\Delta^{199}\text{Hg}$: -0.12‰ in China vs. -0.23‰ in North America and Europe; $P < .05$ by independent samples T-test). Besides the discrepancies of atmospheric Hg chemical and transport cycles, the 1–3 times of atmospheric Hg^0 concentration in China (Fu et al., 2015) is another important cause for these more positive Hg isotopic signatures (Sun et al., 2019a).

Hg in rainfall shows a distinct Hg isotopic composition, with a median of -0.52‰ (mean = $-0.61 \pm 0.43\text{‰}$, $n = 53$), 0.50‰ (mean = $0.54 \pm 0.30\text{‰}$, $n = 53$), and 0.21‰ (mean = $0.22 \pm 0.12\text{‰}$, $n = 53$) for $\delta^{202}\text{Hg}$, $\Delta^{199}\text{Hg}$ and $\Delta^{200}\text{Hg}$, respectively. The Hg isotopic composition of PBM (particle bounded mercury in atmosphere) has the similar direction to Hg in rainfall, but with a more negative median $\delta^{202}\text{Hg}$ of -0.94‰ (mean = $-1.00 \pm 0.49\text{‰}$, $n = 128$), and more positive $\Delta^{199}\text{Hg}$ of 0.31‰ (mean = $0.40 \pm 0.36\text{‰}$, $n = 128$) and $\Delta^{200}\text{Hg}$ of 0.08‰ (mean = $0.08 \pm 0.46\text{‰}$, $n = 128$), respectively. The even-MIF signatures in PBM and rainfall have been proposed to derive from the Hg oxidation processes in the upper atmosphere (Chen et al., 2012; Sun et al., 2016, 2019a). A wide variety of physical, chemical and biological processes are capable of inducing Hg-MDF. In contrast, only photo-reduction and organic matters mediated dark redox can lead to significant Hg-MIF (Blum et al., 2014; Zheng et al., 2019; Zheng & Hintelmann, 2010). Hence, the unique Hg-MIF signatures of the air Hg^0 and Hg^{2+} forms (rainfall Hg and PBM) provide useful signals in tracing the fate of atmospheric Hg depositions in forests.

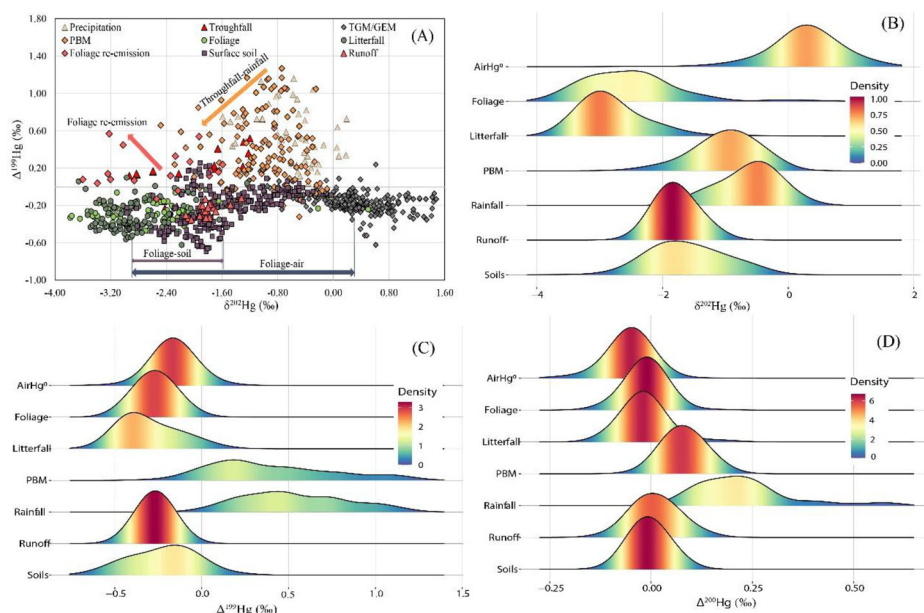


Figure 7. Mercury isotopic compositions in forest ecosystems. (A) the $\delta^{202}\text{Hg}$ vs. $\Delta^{199}\text{Hg}$, (B) the kernel density estimation for $\delta^{202}\text{Hg}$, (C) the kernel density estimation for $\Delta^{199}\text{Hg}$, (D) the kernel density estimation for $\Delta^{200}\text{Hg}$ in each component of the forest ecosystems. The double-head arrow in (A) represents the Hg isotopic fractionation, and the single-head arrow means the direction of the Hg isotopic shifts.

The Hg-MIF signatures of foliage Hg differ from the signatures of atmospheric Hg²⁺, but are close to the signatures of atmospheric Hg⁰, suggesting that the Hg in foliage is primarily through the uptake of atmospheric Hg⁰ (Blum et al., 2014; Demers et al., 2013a; Sonke, 2011). The foliage Hg isotopic composition shows small differences among the different tree species and forest types. Foliage uptake of atmospheric Hg⁰ leads to an average of -2.8‰ of MDF globally, thus global foliage with median $\delta^{202}\text{Hg}$ of -2.57‰ , and -2.17‰ for North America and Europe foliage and -2.78‰ for China foliage. The $\Delta^{199}\text{Hg}$ of foliage is 0.1‰ more negative than the value of air Hg⁰ (median: -0.27‰ vs. -0.17‰), but $\Delta^{200}\text{Hg}$ of foliage is comparable to the value of the air Hg⁰ (median: -0.04‰ vs. -0.03‰). The litterfall $\delta^{202}\text{Hg}$ shows a -0.3‰ to -0.4‰ shift compared to the foliage $\delta^{202}\text{Hg}$ (median: -2.94‰ vs. -2.57‰), and its $\Delta^{199}\text{Hg}$ displays a -0.05‰ to -0.1‰ shift (median: -0.37‰ vs. -0.27‰). Yuan et al. (2019b) has reported that upon Hg⁰ uptake, maturing foliage becomes progressively enriched in lighter Hg isotopes and depleted in odd mass isotopes, which caused by Hg⁰ re-emission (with more negative $\delta^{202}\text{Hg}$ but positive $\Delta^{199}\text{Hg}$ in Fig. 7A) from Hg previously metabolized and bound in the leaf interior after reduction. The re-emission Hg accounts for 30% of the total uptake of Hg (Yuan et al., 2019b).

4.2. Hg accumulation processes on forest floor

Earlier mass balance studies found that the atmospheric Hg deposition shifted from the litterfall Hg deposition in low elevation forests to wet and cloud water induced atmospheric Hg²⁺ deposition in alpine forests (i.e., “cold trapping effect,” Fig. 1), and suggested that Hg deposition caused by the “cold trapping effect” is the dominant deposition pathway for Hg accumulation in surface soil of elevated montane regions (Blackwell & Driscoll, 2015; Lawson et al., 2003; Stankwitz et al., 2012). However, recent studies in montane forests have demonstrated that vegetation uptake of atmospheric Hg⁰ induced Hg deposition (atmospheric Hg⁰ dry deposition) is the main pathway for Hg sources on forest floor, and precipitation and temperature show an indirect effect by

controlling the vegetation biomass and litter decomposition to influence the Hg accumulation in surface soil (Demers et al., 2013a; Guédron et al., 2018; Jiskra et al., 2015; Wang et al., 2017a, 2019d, 2020a, 2020b; Yuan et al., 2019a; Zheng et al., 2016). Global forest surface soil in Fig. 7(C) and 7(D) exhibits a median of -0.20‰ (mean = $-0.22 \pm 0.19\text{‰}$, $n = 320$) $\Delta^{199}\text{Hg}$ value and close to zero $\Delta^{200}\text{Hg}$, both characteristic of the MIF signatures in foliage and litterfall. This confirms the dominant contribution from the atmospheric Hg^0 dry deposition. Using the isotopic fingerprints and statistical modeling, it has been found that both climate and vegetation changes can alter atmospheric Hg^0 dry deposition onto surface soil in forests and therefore change the accumulation and spatial distribution of Hg in soil at the continental scale (Wang et al., 2019c, 2020a).

After the litterfall Hg deposition, Hg in soil is subject to microbial reduction during the initial litter decomposition period, as well as weak yet continuous photo-reduction because the canopy shading constrains sunlight reaching into the forest floor (Wang et al., 2016b; Yuan et al., 2020). Since microbial reduction mainly induced the Hg-MDF, the $\delta^{202}\text{Hg}$ of decomposing litter becomes more positive and the $\Delta^{199}\text{Hg}$ nearly has a small variation (Lu et al., 2021; Yuan et al., 2020). The dark redox reactions mediated by organic matter and microbial reduction become the predominant processes in a time scale of decades to centuries. These reductions lead to a gradually more positive $\delta^{202}\text{Hg}$ in organic soil. In addition, the organic matter induced Hg dark redox transformation has a distinct nuclear volume effect (NVE) that leads to a more negative $\Delta^{199}\text{Hg}$, up to -0.1‰ to -0.3‰ shift between the Oa (i.e., well decomposed humus soil) and litters (Guédron et al., 2018; Jiskra et al., 2015; Lu et al., 2021; Yuan et al., 2019a). Photochemical reduction of Hg^{2+} widely occurs in the environment. Air, foliage and litterfall samples typically exhibit the magnetic isotope effect (MIE) induced a slope of 1 for $\Delta^{199}\text{Hg}$ versus $\Delta^{201}\text{Hg}$ (Bergquist & Blum, 2007; Blum et al., 2020; Sonke, 2011). In deep organic soil, the occurrence of organic matter mediated Hg dark redox alter the slope to slightly greater than 1 due to partial NVE yielding of up a slope of ~ 1.6 (Guédron et al., 2018; Jiskra et al., 2015; Lu et al., 2021; Yuan et al., 2019a). In mineral and deeper soil, with the mixing of Hg derived from geogenic sources (i.e., rock weathering), the $\Delta^{199}\text{Hg}$ gradually become ~ 0 because of diminutive $\Delta^{199}\text{Hg}$ signatures in rocks (Blum et al., 2014; Guédron et al., 2018; Smith et al., 2008; Sun et al., 2019a).

Demers et al. (2013a) reported the isotopic composition of Hg^0 evaded from forest floor and proposed that the Hg^0 evasion may be from air-surface exchange of atmospheric Hg^0 rather than from the emission of legacy Hg on forest floor. However, more field observations suggest occurrence of legacy Hg re-emission based on the strong Hg^0 evasion during daytime and deposition at night (Agnan et al., 2016; Zhu et al., 2016). Jiskra et al. (2019) showed a lower $\delta^{202}\text{Hg}$ and higher $\Delta^{199}\text{Hg}$ in soil pore gas Hg^0 compared to the values in atmospheric Hg^0 , which are attributed to the abiotic oxidation of atmospheric Hg^0 by organic matter in soil. More studies are required to comprehensively understand the contribution of microbial reduction, organic matter redox and photo-reduction induced Hg re-emission from the forest floor.

4.3. Sources of Hg in hydrological transport

Throughfall Hg shows signals of atmospheric Hg^{2+} inputs and atmospheric Hg^{2+} dry deposition which has been represented as the difference between rainfall Hg and throughfall Hg depositions (Demers et al., 2007; Fu et al., 2010; Grigal, 2003; St Louis et al., 2001, 2019; Wang et al., 2009, 2016a). However, the Hg isotopic studies reveal that such difference cannot be solely explained by the atmospheric Hg^{2+} dry deposition. Wang et al. (2020b) reported throughfall Hg isotopic composition in a deglaciated forest chronosequence. They found that $\Delta^{199}\text{Hg}$ and $\Delta^{200}\text{Hg}$ of throughfall are both significantly more negative than those in precipitation, and shifted toward the signatures more characteristic of vegetation covers. Using Hg MIF mixing modeling, it is shown that throughfall Hg contains large ratio of atmospheric Hg^0 sources derived from detritus

of canopy and the canopy epiphyte cover (Wang et al., 2020b). Several studies in forests with Hg isotope data during runoff (Jiskra et al., 2017; Tsui et al., 2020; Woerndle et al., 2018) suggest that runoff would not lead a Hg-MDF because Hg desorbed from soil or decomposed litter is bound to DOM in runoff water, and >70% of the Hg comes from the dry deposition of atmospheric Hg⁰ (Fig. 7) (Jiskra et al., 2017; Tsui et al., 2020; Woerndle et al., 2018).

4.4. Sources of Hg in woods

It has been shown that Hg sources in aboveground woods are mainly from the translocation of foliage uptake of atmospheric Hg⁰ (Sun et al., 2017; Wang et al., 2020b, 2021b). The translocation of foliage uptake of atmospheric Hg⁰ even contributes 44–83% of Hg in roots (Wang et al., 2020b). Wang et al. (2021b) analyzed Hg isotopic compositions in tree-ring profiles, and reported $\delta^{202}\text{Hg}$ values vary among the tree samples, which was attributed to the complexity of Hg-MDF during atmospheric Hg uptake and translocation in vegetation. The $\Delta^{199}\text{Hg}$ signature, which only influenced by the radial translocation in xylem, can be as a tracer to reconstruct a decadal-scale temporal trend of the atmospheric Hg⁰. Overall, woody biomass represents atmospheric Hg⁰ sink underestimated by earlier assessments that focused on litterfall deposition.

5. Summary and implications for the Minamata convention

Knowledge in the biogeochemical cycling of Hg has advanced extensively in the last three decades. Part of the development was leveraged on the advancement of stable Hg isotope techniques capable of tracing sources and processes. Vegetation uptake of atmospheric Hg⁰ is the largest atmospheric Hg⁰ sink in terrestrial ecosystems, and plays an important role in changing the seasonal atmospheric Hg concentration and its isotopic composition, as well as surface soil Hg concentration (Fu et al., 2019; Jiskra et al., 2018; Wang et al., 2019c; Zhou et al., 2021). The quantity of atmospheric Hg deposition mediated by forests (2200–3400 Mg yr⁻¹ including throughfall and vascular/non-vascular vegetation uptake) represents the most important mass budget of Hg in global context.

Earlier studies have intensively focused on the Hg biogeochemical processes in forest soil. To current, the Hg transport and transformation during the forest hydrological processes require more attention. Globally, rainfall Hg deposition is in the range of 690–1000 Mg yr⁻¹ with positive $\Delta^{199}\text{Hg}$ and $\Delta^{200}\text{Hg}$. The absence of atmospheric Hg²⁺ isotope signatures in forest components raises the question on the fate of Hg²⁺ deposition in forests. Atmospheric deposition of Hg²⁺ through precipitation tend to have higher mobility and therefore possibly be diluted by Hg mass from other sources (e.g., geological Hg), removed by groundwater discharge, or re-emitted into atmosphere through chemical or biological reduction (Amos et al., 2015; Grigal, 2002; Lindberg et al., 2007). More studies are needed to identify the fate of Hg in the hydrological processes.

In addition, throughfall and woods contain a large fraction of Hg originated from atmospheric Hg⁰, which was underestimated in earlier assessment. The role of root and canopy epiphyte cover, such as moss and lichen that take up atmospheric Hg⁰ (Wang et al., 2019b) also need attention. A preliminary estimate of Hg uptake by moss covers in forest ecosystems reaches $630 \pm 315\text{ Mg yr}^{-1}$ (Wang et al., 2020b), equivalent to half of the global litterfall Hg deposition (Fu et al., 2016; Wang et al., 2016a), which requires further verification.

The impacts of forest ecosystems on the global Hg cycle depend to a large extent on how changing landuse, both intentionally (e.g., afforestation and deforestation) and unintentionally related to (e.g., climate change) need further assessment (Bishop et al., 2020; Obrist et al., 2018). Accelerated climate change increases the unpredictability of Hg accumulation in forest ecosystems. Extreme drought and wildfire emission of Hg caused by human activities are estimated to be 200–610 Mg yr⁻¹. Climate change alone could increase wildfire Hg emission by 14% globally

in 2050 (Kumar et al., 2018; Outridge et al., 2018; Webster et al., 2016). Wildfire drives emission of Hg on forest floor accumulated over decades to centuries immediately into the atmosphere and increase the local and regional Hg loading, posing substantial ecological risks (Garcia & Carignan, 2005; Kelly et al., 2006; Vijayaraghavan et al., 2014). The ongoing change of landcover and forestry can potentially increase the soil Hg and MeHg transport into the downstream aquatic ecosystems and Hg⁰ re-emission (de Wit et al., 2014; Eklof et al., 2013, 2014; Kronberg et al., 2016; Mazur et al., 2014). These findings have not considered the role of tropical forest ecosystems where 60–70% of global surface Hg storage reside (Wang et al., 2016a, 2019c). The ongoing deforestation is also a concern. It has been estimated that gaseous Hg emissions from soil following forest loss and land change in tropical forests of Brazil is about 4 times greater than in temperate deciduous forest (Carpi et al., 2014). Finally, the recent afforestation in China (27% increase of forest covers in the past two decades) driven by the national ecological projects could have significantly increased the terrestrial Hg sink. More studies are needed to understand the impacts of these human activities on global Hg cycling.

Reduction of anthropogenic Hg emissions mandated by the Minamata Convention will continue to decrease the Hg concentration in the atmosphere. However, it may take a much longer period to observe the response in forest ecosystems. Current studies in aquatic ecosystems suggest that Hg decrease and recovery is slow (up to centennial scale) due to the complex processes associated with climate change and changes in land-use and ecosystems (Braune et al., 2016; Burgess et al., 2013; Evans et al., 2013; Wang et al., 2019a). Recent studies have revealed up to 10⁶ to 10⁷ of magnification for MeHg via the food chain from soil to birds in forest ecosystem (Luo et al., 2020; Sauer et al., 2020; Townsend et al., 2013, 2014; Tsui et al., 2018). This suggests that the forest biota can be as the hotspot for MeHg bioaccumulation which used to occur in the aquatic ecosystems, and we recommend further assessments in these issues. Overall, how quickly terrestrial ecosystems transfer anthropogenic Hg into food webs or back to the atmosphere would affect the global cycling of Hg and risk of Hg exposure to human and wildlife, and thus ultimately determine effects of how actions in accordance with the Minamata Convention.

Disclosure statement

The authors declare no competing financial interest.

Funding

This work was funded by National Natural Science Foundation of China (41977272, 41829701, and 41921004) and K.C. Wong Education Foundation.

ORCID

Xinbin Feng  <http://orcid.org/0000-0002-7462-8998>

References

- Agnan, Y., Le Dantec, T., Moore, C. W., Edwards, G. C., & Obrist, D. (2016). New constraints on terrestrial surface-atmosphere fluxes of gaseous elemental mercury using a global database. *Environmental Science & Technology*, 50(2), 507–524. <https://doi.org/10.1021/acs.est.5b04013>
- Allan, C. J., Heyes, A., Roulet, N. T., St Louis, V. L., & Rudd, J. W. M. (2001). Spatial and temporal dynamics of mercury in Precambrian Shield upland runoff. *Biogeochemistry*, 52(1), 13–40. <https://doi.org/10.1023/A:1026543418120>
- Amado Filho, G. M., Andrade, L. R., Farina, M., & Malm, O. (2002). Hg localisation in *Tillandsia usneoides* L. (Bromeliaceae), an atmospheric biomonitor. *Atmospheric Environment*, 36(5), 881–887. [https://doi.org/10.1016/S1352-2310\(01\)00496-4](https://doi.org/10.1016/S1352-2310(01)00496-4)

- Amos, H. M., Sonke, J. E., Obrist, D., Robins, N., Hagan, N., Horowitz, H. M., Mason, R. P., Witt, M., Hedgecock, I. M., Corbitt, E. S., & Sunderland, E. M. (2015). Observational and modeling constraints on global anthropogenic enrichment of mercury. *Environmental Science & Technology*, 49(7), 4036–4047. <https://doi.org/10.1021/es5058665>
- Arnold, J., Gustin, M. S., & Weisberg, P. J. (2018). Evidence for nonstomatal uptake of Hg by aspen and translocation of hg from foliage to tree rings in Austrian pine. *Environmental Science & Technology*, 52(3), 1174–1182. <https://doi.org/10.1021/acs.est.7b04468>
- Bergquist, B. A., & Blum, J. D. (2007). Mass-dependent and -independent fractionation of Hg isotopes by photoreduction in aquatic systems. *Science (New York, N.Y.)*, 318(5849), 417–420. <https://doi.org/10.1126/science.1148050>
- Bishop, K. H., Lee, Y. H., Munthe, J., & Dambrine, E. (1998). Xylem sap as a pathway for total mercury and methylmercury transport from soils to tree canopy in the boreal forest. *Biogeochemistry*, 40(2/3), 101–113. <https://doi.org/10.1023/A:1005983932240>
- Bishop, K., Shanley, J. B., Riscassi, A., de Wit, H. A., Eklöf, K., Meng, B., Mitchell, C., Osterwalder, S., Schuster, P. F., Webster, J., & Zhu, W. (2020). Recent advances in understanding and measurement of mercury in the environment: Terrestrial Hg cycling. *The Science of the Total Environment*, 721, 137647. <https://doi.org/10.1016/j.scitotenv.2020.137647>
- Blackwell, B. D., & Driscoll, C. T. (2015). Deposition of mercury in forests along a montane elevation gradient. *Environmental Science & Technology*, 49(9), 5363–5370. <https://doi.org/10.1021/es505928w>
- Blum, J. D., & Bergquist, B. A. (2007). Reporting of variations in the natural isotopic composition of mercury. *Analytical and Bioanalytical Chemistry*, 388(2), 353–359. <https://doi.org/10.1007/s00216-007-1236-9>
- Blum, J. D., Drazen, J. C., Johnson, M. W., Popp, B. N., Motta, L. C., & Jamieson, A. J. (2020). Mercury isotopes identify near-surface marine mercury in deep-sea trench biota. *Proceedings of the National Academy of Sciences of the United States of America*, 117(47), 29292–29298. <https://doi.org/10.1073/pnas.2012773117>
- Blum, J. D., Sherman, L. S., & Johnson, M. W. (2014). Mercury Isotopes in Earth and Environmental Sciences. *Annual Review of Earth and Planetary Sciences*, 42(1), 249–269. <https://doi.org/10.1146/annurev-earth-050212-124107>
- Braune, B. M., Gaston, A. J., & Mallory, M. L. (2016). Temporal trends of mercury in eggs of five sympatrically breeding seabird species in the Canadian Arctic. *Environmental Pollution (Barking, Essex: 1987)*, 214, 124–131. <https://doi.org/10.1016/j.envpol.2016.04.006>
- Burgess, N. M., Bond, A. L., Hebert, C. E., Neugebauer, E., & Champoux, L. (2013). Mercury trends in herring gull (*Larus argentatus*) eggs from Atlantic Canada, 1972–2008: Temporal change or dietary shift? *Environmental Pollution (Barking, Essex: 1987)*, 172, 216–222. <https://doi.org/10.1016/j.envpol.2012.09.001>
- Bushey, J. T., Driscoll, C. T., Mitchell, M. J., Selvendiran, P., & Montesdeoca, M. R. (2008). Mercury transport in response to storm events from a northern forest landscape. *Hydrological Processes*, 22(25), 4813–4826. <https://doi.org/10.1002/hyp.7091>
- Carpi, A., Fostier, A. H., Orta, O. R., dos Santos, J. C., & Gittings, M. (2014). Gaseous mercury emissions from soil following forest loss and land use changes: Field experiments in the United States and Brazil. *Atmospheric Environment*, 96, 423–429. <https://doi.org/10.1016/j.atmosenv.2014.08.004>
- Chellman, N., Csank, A., Gustin, M. S., Arienzo, M. M., Vargas Estrada, M., & McConnell, J. R. (2020). Comparison of co-located ice-core and tree-ring mercury records indicates potential radial translocation of mercury in whitebark pine. *The Science of the Total Environment*, 743, 140695. <https://doi.org/10.1016/j.scitotenv.2020.140695>
- Chen, J. B., Hintelmann, H., Feng, X. B., & Dimock, B. (2012). Unusual fractionation of both odd and even mercury isotopes in precipitation from Peterborough, ON, Canada. *Geochimica Et Cosmochimica Acta*, 90, 33–46. <https://doi.org/10.1016/j.gca.2012.05.005>
- Clackett, S. P., Porter, T. J., & Lehnher, I. (2018). 400-year record of atmospheric mercury from tree-rings in northwestern Canada. *Environmental Science & Technology*, 52(17), 9625–9633. <https://doi.org/10.1021/acs.est.8b01824>
- Cui, L. W., Feng, X. B., Lin, C. J., Wang, X. M., Meng, B., Wang, X., & Wang, H. (2014). Accumulation and translocation of 198Hg in four crop species. *Environmental Toxicology and Chemistry*, 33(2), 334–340. <https://doi.org/10.1002/etc.2443>
- de Wit, H. A., Granhus, A., Lindholm, M., Kainz, M. J., Lin, Y., Braaten, H. F. V., & Blaszcak, J. (2014). Forest harvest effects on mercury in streams and biota in Norwegian boreal catchments. *Forest Ecology and Management*, 324, 52–63. <https://doi.org/10.1016/j.foreco.2014.03.044>
- Demers, J. D., Blum, J. D., & Zak, D. R. (2013a). Mercury isotopes in a forested ecosystem: Implications for air-surface exchange dynamics and the global mercury cycle. *Global Biogeochemical Cycles*, 27(1), 222–238. <https://doi.org/10.1002/gbc.20021>

- Demers, J. D., Driscoll, C. T., Fahey, T. J., & Yavitt, J. B. (2007). Mercury cycling in litter and soil in different forest types in the Adirondack region, New York, USA. *Ecological Applications*, 17(5), 1341–1351. <https://doi.org/10.1890/06-1697.1>
- Demers, J. D., Yavitt, J. B., Driscoll, C. T., & Montesdeoca, M. R. (2013b). Legacy mercury and stoichiometry with C, N, and S in soil, pore water, and stream water across the upland-wetland interface: The influence of hydrogeologic setting. *Journal of Geophysical Research: Biogeosciences*, 118(2), 825–841. <https://doi.org/10.1002/jgrg.20066>
- Eklof, K., Kraus, A., Weyhenmeyer, G. A., Meili, M., & Bishop, K. (2012). Forestry influence by stump harvest and site preparation on methylmercury, total mercury and other stream water chemistry parameters across a boreal landscape. *Ecosystems*, 15(8), 1308–1320. <https://doi.org/10.1007/s10021-012-9586-3>
- Eklof, K., Meili, M., Akerblom, S., von Bromssen, C., & Bishop, K. (2013). Impact of stump harvest on run-off concentrations of total mercury and methylmercury. *Forest Ecology and Management*, 290, 83–94. <https://doi.org/10.1016/j.foreco.2012.05.039>
- Eklof, K., Schelker, J., Sorensen, R., Meili, M., Laudon, H., von Bromssen, C., & Bishop, K. (2014). Impact of forestry on total and methylmercury in surface waters: Distinguishing effects of logging and site preparation. *Environmental Science & Technology*, 48(9), 4690–4698. <https://doi.org/10.1021/es404879p>
- Ericksen, J. A., Gustin, M. S., Schorran, D. E., Johnson, D. W., Lindberg, S. E., & Coleman, J. S. (2003). Accumulation of atmospheric mercury in forest foliage. *Atmospheric Environment*, 37(12), 1613–1622. [https://doi.org/10.1016/S1352-2310\(03\)00008-6](https://doi.org/10.1016/S1352-2310(03)00008-6)
- Evans, M., Muir, D., Brua, R. B., Keating, J., & Wang, X. (2013). Mercury trends in predatory fish in Great Slave Lake: The influence of temperature and other climate drivers. *Environmental Science & Technology*, 47(22), 12793–12801. <https://doi.org/10.1021/es402645x>
- Feng, X. B., Foucher, D., Hintelmann, H., Yan, H. Y., He, T. R., & Qiu, G. L. (2010). Tracing mercury contamination sources in sediments using mercury isotope compositions. *Environmental Science & Technology*, 44(9), 3363–3368. <https://doi.org/10.1021/es9039488>
- Frescholtz, T. F., Gustin, M. S., Schorran, D. E., & Fernandez, G. C. J. (2003). Assessing the source of mercury in foliar tissue of quaking aspen. *Environmental Toxicology and Chemistry*, 22(9), 2114–2119. <https://doi.org/10.1002/etc.5620220922>
- Fu, X. W., Feng, X. B., Zhu, W. Z., Rothenberg, S., Yao, H., & Zhang, H. (2010). Elevated atmospheric deposition and dynamics of mercury in a remote upland forest of southwestern China. *Environmental Pollution (Barking, Essex: 1987)*, 158(6), 2324–2333. <https://doi.org/10.1016/j.envpol.2010.01.032>
- Fu, X., Zhang, H., Liu, C., Zhang, H., Lin, C. J., & Feng, X. (2019). Significant seasonal variations in isotopic composition of atmospheric total gaseous mercury at forest sites in China caused by vegetation and mercury sources. *Environmental Science & Technology*, 53(23), 13748–13756. <https://doi.org/10.1021/acs.est.9b05016>
- Fu, X. W., Zhang, H., Yu, B., Wang, X., Lin, C. J., & Feng, X. B. (2015). Observations of atmospheric mercury in China: A critical review. *Atmospheric Chemistry and Physics*, 15(16), 9455–9476. <https://doi.org/10.5194/acp-15-9455-2015>
- Fu, X., Zhu, W., Zhang, H., Sommar, J., Yu, B., Yang, X., Wang, X., Lin, C.-J., & Feng, X. (2016). Depletion of atmospheric gaseous elemental mercury by plant uptake at Mt. Changbai, Northeast China. *Atmospheric Chemistry and Physics*, 16(20), 12861–12873. <https://doi.org/10.5194/acp-16-12861-2016>
- Gabriel, M. C., Williamson, D. G., Brooks, S., Zhang, H., & Lindberg, S. (2005). Spatial variability of mercury emissions from soils in a southeastern US urban environment. *Environmental Geology*, 48(7), 955–964. <https://doi.org/10.1007/s00254-005-0043-x>
- Garcia, E., & Carignan, R. (2005). Mercury concentrations in fish from forest harvesting and fire-impacted Canadian boreal lakes compared using stable isotopes of nitrogen. *Environmental Toxicology and Chemistry*, 24(3), 685–693. <https://doi.org/10.1897/04-065R.1>
- Ghotra, A., Lehnher, I., Porter, T. J., & Pisaric, M. F. J. (2020). Tree-ring inferred atmospheric mercury concentrations in the Mackenzie Delta (NWT, Canada) peaked in the 1970s but are increasing once more. *ACS Earth and Space Chemistry*, 4(3), 457–466. <https://doi.org/10.1021/acsearthspacechem.0c00003>
- Godbold, D. L., & Huttermann, A. (1985). Effect of zinc, cadmium and mercury on root elongation of *Picea-abies* (Karst) seedlings, and the significance of these metals to forest dieback. *Environmental Pollution Series a-Ecological and Biological*, 38(4), 375–381. [https://doi.org/10.1016/0143-1471\(85\)90108-4](https://doi.org/10.1016/0143-1471(85)90108-4)
- Gong, P., Wang, X. P., Xue, Y. G., Xu, B. Q., & Yao, T. D. (2014). Mercury distribution in the foliage and soil profiles of the Tibetan forest: Processes and implications for regional cycling. *Environmental Pollution (Barking, Essex: 1987)*, 188, 94–101. <https://doi.org/10.1016/j.envpol.2014.01.020>
- Graydon, J. A., Louis, V. L. S., Hintelmann, H., Lindberg, S. E., Sandilands, K. A., Rudd, J. W. M., Kelly, C. A., Hall, B. D., & Mowat, L. D. (2008). Long-term wet and dry deposition of total and methyl mercury in the remote boreal ecoregion of Canada. *Environmental Science & Technology*, 42(22), 8345–8351. <https://doi.org/10.1021/es801056j>

- Graydon, J. A., St Louis, V. L., Hintelmann, H., Lindberg, S. E., Sandilands, K. A., Rudd, J. W., Kelly, C. A., Tate, M. T., Krabbenhoft, D. P., & Lehnher, I. (2009). Investigation of uptake and retention of atmospheric Hg(II) by boreal forest plants using stable Hg isotopes. *Environmental Science & Technology*, 43(13), 4960–4966. <https://doi.org/10.1021/es900357s>
- Greger, M., Wang, Y., & Neuschutz, C. (2005). Absence of Hg transpiration by shoot after Hg uptake by roots of six terrestrial plant species. *Environmental Pollution (Barking, Essex: 1987)*, 134(2), 201–208. <https://doi.org/10.1016/j.envpol.2004.08.007>
- Grigal, D. F. (2002). Inputs and outputs of mercury from terrestrial watersheds: A review. *Environmental Reviews*, 10(1), 1–39. <https://doi.org/10.1139/a01-013>
- Grigal, D. F. (2003). Mercury sequestration in forests and peatlands: A review. *Journal of Environmental Quality*, 32(2), 393–405. <https://doi.org/10.2134/jeq2003.3930>
- Guédron, S., Amouroux, D., Tessier, E., Grimaldi, C., Barre, J., Berail, S., Perrot, V., & Grimaldi, M. (2018). Mercury isotopic fractionation during pedogenesis in a tropical forest soil catena (French Guiana): Deciphering the impact of historical gold mining. *Environmental Science & Technology*, 52, 11573–11582.
- Gustin, M. S., Lindberg, S., Marsik, F., Casimir, A., Ebinghaus, R., Edwards, G., Hubble-Fitzgerald, C., Kemp, R., Kock, H., Leonard, T., London, J., Majewski, M., Montecinos, C., Owens, J., Pilote, M., Poissant, L., Rasmussen, P., Schaedlich, F., Schneeberger, D., ... Zhang, H. (1999). Nevada STORMS project: Measurement of mercury emissions from naturally enriched surfaces. *Journal of Geophysical Research: Atmospheres*, 104(D17), 21831–21844. <https://doi.org/10.1029/1999JD900351>
- Hanson, P. J., Lindberg, S. E., Tabberer, T. A., Owens, J. G., & Kim, K. H. (1995). Foliar exchange of mercury-vapor - evidence for a compensation point. *Water, Air, & Soil Pollution*, 80(1–4), 373–382. <https://doi.org/10.1007/BF01189687>
- Hanson, P. J., Tabberer, T. A., & Lindberg, S. E. (1997). Emissions of mercury vapor from tree bark. *Atmospheric Environment*, 31(5), 777–780. [https://doi.org/10.1016/S1352-2310\(96\)00231-2](https://doi.org/10.1016/S1352-2310(96)00231-2)
- Hultberg, H., Munthe, J., & Iverfeldt, A. (1995). Cycling of methyl mercury and mercury - responses in the forest roof catchment to 3 years of decreased atmospheric deposition. *Water Air and Soil Pollution*, 80, 415–424. <https://doi.org/10.1007/BF01189691>
- Jiskra, M., Sonke, J. E., Agnan, Y., Helmig, D., & Obrist, D. (2019). Insights from mercury stable isotopes on terrestrial-atmosphere exchange of Hg(0) in the Arctic tundra. *Biogeosciences*, 16(20), 4051–4064. <https://doi.org/10.5194/bg-16-4051-2019>
- Jiskra, M., Sonke, J. E., Obrist, D., Bieser, J., Ebinghaus, R., Myhre, C. L., Pfaffhuber, K. A., Wangberg, I., Kyllonen, K., Worthy, D., Martin, L. G., Labuschagne, C., Mkololo, T., Ramonet, M., Magand, O., & Dommergue, A. (2018). A vegetation control on seasonal variations in global atmospheric mercury concentrations. *Nature Geoscience*, 11(4), 244–250. <https://doi.org/10.1038/s41561-018-0078-8>
- Jiskra, M., Wiederhold, J. G., Skyllberg, U., Kronberg, R.-M., Hajdas, I., & Kretzschmar, R. (2015). Mercury deposition and re-emission pathways in boreal forest soils investigated with Hg isotope signatures. *Environmental Science & Technology*, 49(12), 7188–7196. <https://doi.org/10.1021/acs.est.5b00742>
- Jiskra, M., Wiederhold, J. G., Skyllberg, U., Kronberg, R. M., & Kretzschmar, R. (2017). Source tracing of natural organic matter bound mercury in boreal forest runoff with mercury stable isotopes. *Environmental Science. Processes & Impacts*, 19(10), 1235–1248. <https://doi.org/10.1039/c7em00245a>
- Kelly, E. N., Schindler, D. W., St Louis, V. L., Donald, D. B., & Vladicka, K. E. (2006). Forest fire increases mercury accumulation by fishes via food web restructuring and increased mercury inputs. *Proceedings of the National Academy of Sciences of the United States of America*, 103(51), 19380–19385. <https://doi.org/10.1073/pnas.0609798104>
- Kronberg, R.-M., Drott, A., Jiskra, M., Wiederhold, J. G., Bjorn, E., & Skyllberg, U. (2016). Forest harvest contribution to Boreal freshwater methyl mercury load. *Global Biogeochemical Cycles*, 30(6), 825–843. <https://doi.org/10.1002/2015GB005316>
- Kumar, A., Wu, S., Huang, Y., Liao, H., & Kaplan, J. O. (2018). Mercury from wildfires: Global emission inventories and sensitivity to 2000–2050 global change. *Atmospheric Environment*, 173, 6–15. <https://doi.org/10.1016/j.atmosenv.2017.10.061>
- Kwon, S. Y., Blum, J. D., Yin, R., Tsui, M. T.-K., Yang, Y. H., & Choi, J. W. (2020). Mercury stable isotopes for monitoring the effectiveness of the Minamata Convention on Mercury. *Earth-Science Reviews*, 203, 103111. <https://doi.org/10.1016/j.earscirev.2020.103111>
- Laacouri, A., Nater, E. A., & Kolka, R. K. (2013). Distribution and uptake dynamics of mercury in leaves of common deciduous tree species in Minnesota. *Environmental Science & Technology*, 47(18), 10462–10470. <https://doi.org/10.1021/es401357z>
- Lawson, S. T., Scherbatskoy, T. D., Malcolm, E. G., & Keeler, G. J. (2003). Cloud water and throughfall deposition of mercury and trace elements in a high elevation spruce-fir forest at Mt. Mansfield, Vermont. *Journal of Environmental Monitoring: JEM*, 5(4), 578–583. <https://doi.org/10.1039/b210125d>

- Lee, Y. H., Bishop, K. H., & Munthe, J. (2000). Do concepts about catchment cycling of methylmercury and mercury in boreal catchments stand the test of time? Six years of atmospheric inputs and runoff export at Svartberget, northern Sweden. *The Science of the Total Environment*, 260(1–3), 11–20. [https://doi.org/10.1016/S0048-9697\(00\)00538-6](https://doi.org/10.1016/S0048-9697(00)00538-6)
- Lee, Y. H., Bishop, K. H., Munthe, J., Iverfeldt, A., Verta, M., Parkman, H., & Hultberg, H. (1998). An examination of current Hg deposition and export in Fenno-Scandian catchments. *Biogeochemistry*, 40(2/3), 125–135. <https://doi.org/10.1023/A:1005926321337>
- Leonard, T. L., Taylor, G. E., Gustin, M. S., & Fernandez, G. C. J. (1998a). Mercury and plants in contaminated soils: 1. Uptake, partitioning, and emission to the atmosphere. *Environmental Toxicology and Chemistry*, 17(10), 2063–2071. <https://doi.org/10.1002/etc.5620171024>
- Leonard, T. L., Taylor, G. E., Gustin, M. S., & Fernandez, G. C. J. (1998b). Mercury and plants in contaminated soils: 2. Environmental and physiological factors governing mercury flux to the atmosphere. *Environmental Toxicology and Chemistry*, 17(10), 2072–2079. <https://doi.org/10.1002/etc.5620171025>
- Lin, Y., Larssen, T., Vogt, R. D., Feng, X. B., & Zhang, H. (2011). Transport and fate of mercury under different hydrologic regimes in polluted stream in mining area. *Journal of Environmental Sciences*, 23(5), 757–764. [https://doi.org/10.1016/S1001-0742\(10\)60473-1](https://doi.org/10.1016/S1001-0742(10)60473-1)
- Lindberg, S., Bullock, R., Ebinghaus, R., Engstrom, D., Feng, X. B., Fitzgerald, W., Pirrone, N., Prestbo, E., Seigneur, C., & Panel on Source Attribution of Atmospheric Mercury. (2007). A synthesis of progress and uncertainties in attributing the sources of mercury in deposition. *Ambio*, 36(1), 19–32. [https://doi.org/10.1579/0044-7447\(2007\)36\[19:ASOPAU2.0.CO;2\]](https://doi.org/10.1579/0044-7447(2007)36[19:ASOPAU2.0.CO;2])
- Lindberg, S. E., Dong, W. J., & Meyers, T. (2002). Transpiration of gaseous elemental mercury through vegetation in a subtropical wetland in Florida. *Atmospheric Environment*, 36(33), 5207–5219. [https://doi.org/10.1016/S1352-2310\(02\)00586-1](https://doi.org/10.1016/S1352-2310(02)00586-1)
- Lindberg, S. E., Meyers, T. P., & Munthe, J. (1995). Evasion of mercury vapor from tree surface of a recently limed acid forest lake in Sweden. *Water, Air, & Soil Pollution*, 85(2), 725–730. <https://doi.org/10.1007/BF00476915>
- Lu, Z., Yuan, W., Luo, K., & Wang, X. (2021). Litterfall mercury reduction on a subtropical evergreen broadleaf forest floor revealed by multi-element isotopes. *Environmental Pollution (Barking, Essex: 1987)*, 268(Pt A), 115867. <https://doi.org/10.1016/j.envpol.2020.115867>
- Luo, Y., Duan, L., Wang, L., Xu, G. Y., Wang, S. X., & Hao, J. M. (2014). Mercury concentrations in forest soils and stream waters in northeast and south China. *The Science of the Total Environment*, 496, 714–720. <https://doi.org/10.1016/j.scitotenv.2014.07.036>
- Luo, K., Xu, Z., Wang, X., Quan, R.-C., Lu, Z., Bi, W., Zhao, H., & Qiu, G. (2020). Terrestrial methylmercury bioaccumulation in a pine forest food chain revealed by live nest videography observations and nitrogen isotopes. *Environmental Pollution*, 263, 114530. <https://doi.org/10.1016/j.envpol.2020.114530>
- Manceau, A., Lemouchi, C., Enescu, M., Gaillot, A. C., Lanson, M., Magnin, V., Glatzel, P., Poulin, B. A., Ryan, J. N., Aiken, G. R., Gautier-Luneau, I., & Nagy, K. L. (2015). Formation of mercury sulfide from Hg(II)-thiolate complexes in natural organic matter. *Environmental Science & Technology*, 49(16), 9787–9796. <https://doi.org/10.1021/acs.est.5b02522>
- Manceau, A., Wang, J. X., Rovezzi, M., Glatzel, P., & Feng, X. B. (2018). Biogenesis of mercury-sulfur nanoparticles in plant leaves from atmospheric gaseous mercury. *Environmental Science & Technology*, 52(7), 3935–3948. <https://doi.org/10.1021/acs.est.7b05452>
- Mao, H. T., Cheng, I., & Zhang, L. M. (2016). Current understanding of the driving mechanisms for spatiotemporal variations of atmospheric speciated mercury: A review. *Atmospheric Chemistry and Physics*, 16(20), 12897–12924. <https://doi.org/10.5194/acp-16-12897-2016>
- Mazur, M., Mitchell, C. P. J., Eckley, C. S., Eggert, S. L., Kolka, R. K., Sebestyen, S. D., & Swain, E. B. (2014). Gaseous mercury fluxes from forest soils in response to forest harvesting intensity: A field manipulation experiment. *The Science of the Total Environment*, 496, 678–687. <https://doi.org/10.1016/j.scitotenv.2014.06.058>
- Meili, M. (1991a). The coupling of mercury and organic-matter in the biogeochemical cycle - towards a mechanistic model for the boreal forest zone. *Water Air & Soil Pollution*, 56(1), 333–347. <https://doi.org/10.1007/BF00342281>
- Meili, M. (1991b). Fluxes, pools, and turnover of mercury in Swedish forest lakes. *Water Air & Soil Pollution*, 56(1), 719–727. <https://doi.org/10.1007/BF00342312>
- Meng, B., Li, Y., Cui, W., Jiang, P., Liu, G., Wang, Y., Richards, J., Feng, X., & Cai, Y. (2018). Tracing the uptake, transport, and fate of mercury in sawgrass (*Cladium jamaicense*) in the Florida Everglades using a multi-isotope technique. *Environmental Science & Technology*, 52(6), 3384–3391. <https://doi.org/10.1021/acs.est.7b04150>
- Navratil, T., Hojdova, M., Rohovec, J., Penizek, V., & Varilova, Z. (2009). Effect of fire on pools of mercury in forest soil, Central Europe. *Bulletin of Environmental Contamination and Toxicology*, 83(2), 269–274. <https://doi.org/10.1007/s00128-009-9705-9>

- Navratil, T., Shanley, J., Rohovec, J., Hojdova, M., Penizek, V., & Buchtova, J. (2014). Distribution and pools of mercury in Czech forest soils. *Water Air and Soil Pollution*, 225(3), 1829. <https://doi.org/10.1007/s11270-013-1829-1>
- Novakova, T., Navratil, T., Demers, J. D., Roll, M., & Rohovec, J. (2021). Contrasting tree ring Hg records in two conifer species: Multi-site evidence of species-specific radial translocation effects in Scots pine versus European larch. *Science of the Total Environment*, 762, 144022. <https://doi.org/10.1016/j.scitotenv.2020.144022>
- Obrist, D., Fain, X., & Berger, C. (2010). Gaseous elemental mercury emissions and CO₂ respiration rates in terrestrial soils under controlled aerobic and anaerobic laboratory conditions. *The Science of the Total Environment*, 408(7), 1691–1700. <https://doi.org/10.1016/j.scitotenv.2009.12.008>
- Obrist, D., Johnson, D. W., & Lindberg, S. E. (2009). Mercury concentrations and pools in four Sierra Nevada forest sites, and relationships to organic carbon and nitrogen. *Biogeosciences*, 6(5), 765–777. <https://doi.org/10.5194/bg-6-765-2009>
- Obrist, D., Johnson, D. W., Lindberg, S. E., Luo, Y., Hararuk, O., Bracho, R., Battles, J. J., Dail, D. B., Edmonds, R. L., Monson, R. K., Ollinger, S. V., Pallardy, S. G., Pregitzer, K. S., & Todd, D. E. (2011). Mercury distribution across 14 US forests. Part I: Spatial patterns of concentrations in biomass. *Litter, and Soils. Environmental Science, & Technology* 45, 3974–3981.
- Obrist, D., Kirk, J. L., Zhang, L., Sunderland, E. M., Jiskra, M., & Selin, N. E. (2018). A review of global environmental mercury processes in response to human and natural perturbations: Changes of emissions, climate, and land use. *Ambio*, 47(2), 116–140. <https://doi.org/10.1007/s13280-017-1004-9>
- Obrist, D., Pearson, C., Webster, J., Kane, T., Lin, C. J., Aiken, G. R., & Alpers, C. N. (2016). A synthesis of terrestrial mercury in the western United States: Spatial distribution defined by land cover and plant productivity. *The Science of the Total Environment*, 568, 522–535. <https://doi.org/10.1016/j.scitotenv.2015.11.104>
- Outridge, P. M., Mason, R. P., Wang, F., Guerrero, S., & Heimbürger-Boavida, L. E. (2018). Updated global and oceanic mercury budgets for the United Nations Global Mercury Assessment 2018. *Environmental Science & Technology*, 52(20), 11466–11477. <https://doi.org/10.1021/acs.est.8b01246>
- Poissant, L., Pilote, M., Yumvihoze, E., & Lean, D. (2008). Mercury concentrations and foliage/atmosphere fluxes in a maple forest ecosystem in Quebec, Canada. *Journal of Geophysical Research*, 113(D10307), 1–12. <https://doi.org/10.1029/2007JD009510>
- Pokharel, A. K., & Obrist, D. (2011). Fate of mercury in tree litter during decomposition. *Biogeosciences*, 8(9), 2507–2521. <https://doi.org/10.5194/bg-8-2507-2011>
- Rea, A. W., Keeler, G. J., & Scherbatskoy, T. (1996). The deposition of mercury in throughfall and litterfall in the Lake Champlain watershed: A short-term study. *Atmospheric Environment*, 30(19), 3257–3263. [https://doi.org/10.1016/1352-2310\(96\)00087-8](https://doi.org/10.1016/1352-2310(96)00087-8)
- Rea, A. W., Lindberg, S. E., & Keeler, G. J. (2001). Dry deposition and foliar leaching of mercury and selected trace elements in deciduous forest throughfall. *Atmospheric Environment*, 35(20), 3453–3462. [https://doi.org/10.1016/S1352-2310\(01\)00133-9](https://doi.org/10.1016/S1352-2310(01)00133-9)
- Rodríguez Martín, J. A., Gutiérrez, C., Torrijos, M., & Nanos, N. (2018). Wood and bark of *Pinus halepensis* as archives of heavy metal pollution in the Mediterranean Region. *Environmental Pollution (Barking, Essex: 1987)*, 239, 438–447. <https://doi.org/10.1016/j.envpol.2018.04.036>
- Sauer, A. K., Driscoll, C. T., Evers, D. C., Adams, E. M., & Yang, Y. (2020). Mercury exposure in songbird communities within Sphagnum bog and upland forest ecosystems in the Adirondack Park (New York, USA). *Ecotoxicology (London, England)*, 29(10), 1815–1829. <https://doi.org/10.1007/s10646-019-02142-x>
- Scanlon, T. M., Riscassi, A. L., Demers, J. D., Camper, T. D., Lee, T. R., & Druckenbrod, D. L. (2020). Mercury accumulation in tree rings: Observed trends in quantity and isotopic composition in Shenandoah National Park, Virginia. *Journal of Geophysical Research: Biogeosciences*, 125(2), e2019JG005445. <https://doi.org/10.1029/2019JG005445>
- Schneider, L., Allen, K., Walker, M., Morgan, C., & Haberle, S. (2019). Using tree rings to track atmospheric mercury pollution in Australia: The legacy of mining in Tasmania. *Environmental Science & Technology*, 53(10), 5697–5706. <https://doi.org/10.1021/acs.est.8b06712>
- Schwesig, D., & Matzner, E. (2000). Pools and fluxes of mercury and methylmercury in two forested catchments in Germany. *The Science of the Total Environment*, 260(1–3), 213–223. [https://doi.org/10.1016/S0048-9697\(00\)00565-9](https://doi.org/10.1016/S0048-9697(00)00565-9)
- Selin, N. E. (2009). Global biogeochemical cycling of mercury: A review. *Annual Review of Environment and Resources*, 34(1), 43–63. <https://doi.org/10.1146/annurev.enviro.051308.084314>
- Selvendiran, P., Driscoll, C. T., Bushey, J. T., & Montesdeoca, M. R. (2008a). Wetland influence on mercury fate and transport in a temperate forested watershed. *Environmental Pollution (Barking, Essex: 1987)*, 154(1), 46–55. <https://doi.org/10.1016/j.envpol.2007.12.005>
- Selvendiran, P., Driscoll, C. T., Montesdeoca, M. R., & Bushey, J. T. (2008b). Inputs, storage, and transport of total and methyl mercury in two temperate forest wetlands. *Journal of Geophysical Research-Biogeosciences*, 113, G00C01. <https://doi.org/10.1029/2008JG000739>

- Smith, C. N., Kesler, S. E., Blum, J. D., & Rytuba, J. J. (2008). Isotope geochemistry of mercury in source rocks, mineral deposits and spring deposits of the California Coast Ranges, USA. *Earth and Planetary Science Letters*, 269(3–4), 399–406. <https://doi.org/10.1016/j.epsl.2008.02.029>
- Sonke, J. E. (2011). A global model of mass independent mercury stable isotope fractionation. *Geochimica Et Cosmochimica Acta*, 75(16), 4577–4590. <https://doi.org/10.1016/j.gca.2011.05.027>
- Sorensen, R., Meili, M., Lambertsson, L., von Bromssen, C., & Bishop, K. (2009). The effects of forest harvest operations on mercury and methylmercury in two boreal streams: Relatively small changes in the first two years prior to site preparation. *Ambio*, 38(7), 364–372. <https://doi.org/10.1579/0044-7447-38.7.364>
- Spawn, S. A., Sullivan, C. C., Lark, T. J., & Gibbs, H. K. (2020). Harmonized global maps of above and below-ground biomass carbon density in the year 2010. *Scientific Data*, 7(1), 112. <https://doi.org/10.1038/s41597-020-0444-4>
- St Louis, V. L., Graydon, J. A., Lehnher, I., Amos, H. M., Sunderland, E. M., St Pierre, K. A., Emmerton, C. A., Sandilands, K., Tate, M., Steffen, A., & Humphreys, E. R. (2019). Atmospheric concentrations and wet/dry loadings of mercury at the remote experimental Lakes Area, Northwestern Ontario. *Environmental Science & Technology*, 53(14), 8017–8026. <https://doi.org/10.1021/acs.est.9b01338>
- St Louis, V. L., Rudd, J. W. M., Kelly, C. A., Hall, B. D., Rolfhus, K. R., Scott, K. J., Lindberg, S. E., & Dong, W. (2001). Importance of the forest canopy to fluxes of methyl mercury and total mercury to boreal ecosystems. *Environmental Science & Technology*, 35(15), 3089–3098. <https://doi.org/10.1021/es001924p>
- Stamenkovic, J., & Gustin, M. S. (2009). Nonstomatal versus stomatal uptake of atmospheric mercury. *Environmental Science & Technology*, 43(5), 1367–1372. <https://doi.org/10.1021/es801583a>
- Stamenkovic, J., Gustin, M. S., Arnone, J. A., Johnson, D. W., Larsen, J. D., & Verburg, P. S. J. (2008). Atmospheric mercury exchange with a tallgrass prairie ecosystem housed in mesocosms. *The Science of the Total Environment*, 406(1–2), 227–238. <https://doi.org/10.1016/j.scitotenv.2008.07.047>
- Stankwitz, C., Kaste, J. M., & Friedland, A. J. (2012). Threshold increases in soil lead and mercury from tropospheric deposition across an elevational gradient. *Environmental Science & Technology*, 46(15), 8061–8068. <https://doi.org/10.1021/es204208w>
- Streets, D. G., Devane, M. K., Lu, Z. F., Bond, T. C., Sunderland, E. M., & Jacob, D. J. (2011). All-time releases of mercury to the atmosphere from human activities. *Environmental Science & Technology*, 45(24), 10485–10491. <https://doi.org/10.1021/es202765m>
- Streets, D. G., Hao, J. M., Wu, Y., Jiang, J. K., Chan, M., Tian, H. Z., & Feng, X. B. (2005). Anthropogenic mercury emissions in China. *Atmospheric Environment*, 39(40), 7789–7806. <https://doi.org/10.1016/j.atmosenv.2005.08.029>
- Sun, R., Jiskra, M., Amos, H. M., Zhang, Y., Sunderland, E. M., & Sonke, J. E. (2019a). Modelling the mercury stable isotope distribution of Earth surface reservoirs: Implications for global Hg cycling. *Geochimica Et Cosmochimica Acta*, 246, 156–173. <https://doi.org/10.1016/j.gca.2018.11.036>
- Sun, L. M., Lu, B. Y., Yuan, D. X., Hao, W. B., & Zheng, Y. (2017). Variations in the isotopic composition of stable mercury isotopes in typical mangrove plants of the Jiulong estuary, SE China. *Environmental Science and Pollution Research International*, 24(2), 1459–1468. <https://doi.org/10.1007/s11356-016-7933-1>
- Sun, T., Ma, M., Wang, X., Wang, Y., Du, H., Xiang, Y., Xu, Q., Xie, Q., & Wang, D. (2019b). Mercury transport, transformation and mass balance on a perspective of hydrological processes in a subtropical forest of China. *Environmental Pollution (Barking, Essex: 1987)*, 254(Pt B), 113065. <https://doi.org/10.1016/j.envpol.2019.113065>
- Sun, G., Sommar, J., Feng, X., Lin, C.-J., Ge, M., Wang, W., Yin, R., Fu, X., & Shang, L. (2016). Mass-dependent and -independent fractionation of mercury isotope during gas-phase oxidation of elemental mercury vapor by atomic Cl and Br. *Environmental Science & Technology*, 50(17), 9232–9241. <https://doi.org/10.1021/acs.est.6b01668>
- Tang, R. G., Luo, J., She, J., Chen, Y. C., Yang, D. D., & Zhou, J. (2015). The cadmium and lead of soil in timberline coniferous forests. *Environmental Earth Sciences*, 73(1), 303–310. <https://doi.org/10.1007/s12665-014-3424-1>
- Townsend, J. M., Driscoll, C. T., Rimmer, C. C., & McFarland, K. P. (2014). Avian, salamander, and forest floor mercury concentrations increase with elevation in a terrestrial ecosystem. *Environmental Toxicology and Chemistry*, 33(1), 208–215. <https://doi.org/10.1002/etc.2438>
- Townsend, J. M., Rimmer, C. C., Driscoll, C. T., McFarland, K. P., & Inigo-Elias, E. (2013). Mercury concentrations in tropical resident and migrant songbirds on Hispaniola. *Ecotoxicology (London, England)*, 22(1), 86–93. <https://doi.org/10.1007/s10646-012-1005-1>
- Tsui, M. T.-K., Adams, E. M., Jackson, A. K., Evers, D. C., Blum, J. D., & Balogh, S. J. (2018). Understanding sources of methylmercury in songbirds with stable mercury isotopes: Challenges and future directions. *Environmental Toxicology and Chemistry*, 37(1), 166–174. <https://doi.org/10.1002/etc.3941>
- Tsui, M. T., Blum, J. D., & Kwon, S. Y. (2019). Review of stable mercury isotopes in ecology and biogeochemistry. *Science of the Total Environment*, 716, 135386. <https://doi.org/10.1016/j.scitotenv.2019.135386>

- Tsui, M. T. K., Uzun, H., Ruecker, A., Majidzadeh, H., Ulus, Y., Zhang, H., Bao, S., Blum, J. D., Karanfil, T., & Chow, A. T. (2020). Concentration and isotopic composition of mercury in a blackwater river affected by extreme flooding events. *Limnology and Oceanography*, 65(9), 2158–2169. <https://doi.org/10.1002/lno.11445>
- UN-Environment. (2019). *Global Mercury Assessment 2018*. UN-Environment Programme, Chemicals and Health Branch.
- Vidun, P. G., Mitchell, C. P., Jacinthe, P. A., Baker, M. E., Liu, X., & Fisher, K. R. (2013). Mercury dynamics in groundwater across three distinct riparian zone types of the US Midwest. *Environmental Science: Processes & Impacts*, 15(11), 2131–2141. <https://doi.org/10.1039/c3em00254c>
- Vijayaraghavan, K., Levin, L., Parker, L., Yarwood, G., & Streets, D. (2014). Response of fish tissue mercury in a freshwater lake to local, regional, and global changes in mercury emissions. *Environmental Toxicology and Chemistry*, 33(6), 1238–1247. <https://doi.org/10.1002/etc.2584>
- Wang, X., Bao, Z., Lin, C.-J., Yuan, W., & Feng, X. (2016a). Assessment of global mercury deposition through litterfall. *Environmental Science & Technology*, 50(16), 8548–8557. <https://doi.org/10.1021/acs.est.5b06351>
- Wang, J. J., Guo, Y. Y., Guo, D. L., Yin, S. L., Kong, D. L., Liu, Y. S., & Zeng, H. (2012). Fine root mercury heterogeneity: Metabolism of lower-order roots as an effective route for mercury removal. *Environmental Science & Technology*, 46(2), 769–777. <https://doi.org/10.1021/es2018708>
- Wang, X., Lin, C. J., Feng, X. B., Yuan, W., Fu, X. W., Zhang, H., Wu, Q. R., & Wang, S. X. (2018). Assessment of regional mercury deposition and emission outflow in Mainland China. *Journal of Geophysical Research: Atmospheres*, 123(17), 9868–9890. <https://doi.org/10.1029/2018JD028350>
- Wang, X., Lin, C.-J., Lu, Z., Zhang, H., Zhang, Y., & Feng, X. (2016b). Enhanced accumulation and storage of mercury on subtropical evergreen forest floor: Implications on mercury budget in global forest ecosystems. *Journal of Geophysical Research: Biogeosciences*, 121(8), 2096–2109. <https://doi.org/10.1002/2016JG003446>
- Wang, X., Luo, J., Yin, R., Yuan, W., Lin, C.-J., Sommar, J., Feng, X., Wang, H., & Lin, C. (2017a). Using mercury isotopes to understand mercury accumulation in the montane forest floor of the Eastern Tibetan Plateau. *Environmental Science & Technology*, 51(2), 801–809. <https://doi.org/10.1021/acs.est.6b03806>
- Wang, X., Luo, J., Yuan, W., Lin, C. J., Wang, F., Liu, C., Wang, G., & Feng, X. (2020a). Global warming accelerates uptake of atmospheric mercury in regions experiencing glacier retreat. *Proceedings of the National Academy of Sciences of the United States of America*, 117(4), 2049–2055. <https://doi.org/10.1073/pnas.1906930117>
- Wang, F., Outridge, P. M., Feng, X., Meng, B., Heimbürger-Boavida, L. E., & Mason, R. P. (2019a). How closely do mercury trends in fish and other aquatic wildlife track those in the atmosphere? - Implications for evaluating the effectiveness of the Minamata Convention. *The Science of the Total Environment*, 674, 58–70. <https://doi.org/10.1016/j.scitotenv.2019.04.101>
- Wang, T., Yang, G., Du, H., Guo, P., Sun, T., An, S., Wang, D., & Ma, M. (2021a). Migration characteristics and potential determinants of mercury in long-term decomposing litterfall of two subtropical forests. *Ecotoxicology and Environmental Safety*, 208, 111402. <https://doi.org/10.1016/j.ecoenv.2020.111402>
- Wang, X., Yuan, W., & Feng, X. (2017b). Global review of mercury biogeochemical processes in forest ecosystems. *Progress in Chemistry*, 29, 970–980.
- Wang, X., Yuan, W., Feng, X., Wang, D., & Luo, J. (2019b). Moss facilitating mercury, lead and cadmium enhanced accumulation in organic soils over glacial erratic at Mt. Gongga, China. *Environmental Pollution (Barking, Essex: 1987)*, 254(Pt A), 112974. <https://doi.org/10.1016/j.envpol.2019.112974>
- Wang, X., Yuan, W., Lin, C. J., Luo, J., Wang, F., Feng, X., Fu, X., & Liu, C. (2020b). Underestimated sink of atmospheric mercury in a deglaciated forest chronosequence. *Environmental Science & Technology*, 54(13), 8083–8093. <https://doi.org/10.1021/acs.est.0c01667>
- Wang, X., Yuan, W., Lin, C.-J., Wu, F., & Feng, X. (2021b). Stable mercury isotopes stored in Masson Pinus tree rings as atmospheric mercury archives. *Journal of Hazardous Materials*, 415, 125678. <https://doi.org/10.1016/j.jhazmat.2021.125678>
- Wang, X., Yuan, W., Lin, C. J., Zhang, L. M., Zhang, H., & Feng, X. B. (2019c). Climate and vegetation as primary drivers for global mercury storage in surface soil. *Environmental Science & Technology*, 53(18), 10665–10675. <https://doi.org/10.1021/acs.est.9b02386>
- Wang, X., Yuan, W., Lu, Z. Y., Lin, C. J., Yin, R. S., Li, F., & Feng, X. B. (2019d). Effects of precipitation on mercury accumulation on subtropical montane forest floor: Implications on climate forcing. *Journal of Geophysical Research: Biogeosciences*, 124(4), 959–972. <https://doi.org/10.1029/2018JG004809>
- Wang, Z., Zhang, X., Xiao, J., Zhijia, C., & Yu, P. (2009). Mercury fluxes and pools in three subtropical forested catchments, southwest China. *Environmental Pollution (Barking, Essex: 1987)*, 157(3), 801–808. <https://doi.org/10.1016/j.envpol.2008.11.018>
- Webster, J. P., Kane, T. J., Obrist, D., Ryan, J. N., & Aiken, G. R. (2016). Estimating mercury emissions resulting from wildfire in forests of the Western United States. *Science of the Total Environment*, 568, 578–586. <https://doi.org/10.1016/j.scitotenv.2016.01.166>

- Woerndle, G. E., Tsz-Ki Tsui, M., Sebestyen, S. D., Blum, J. D., Nie, X., & Kolka, R. K. (2018). New insights on ecosystem mercury cycling revealed by stable isotopes of mercury in water flowing from a headwater peatland catchment. *Environmental Science & Technology*, 52(4), 1854–1861. <https://doi.org/10.1021/acs.est.7b04449>
- Wu, Q., Wang, S., Li, G., Liang, S., Lin, C.-J., Wang, Y., Cai, S., Liu, K., & Hao, J. (2016). Temporal trend and spatial distribution of speciated atmospheric mercury emissions in China during 1978–2014. *Environmental Science & Technology*, 50(24), 13428–13435. <https://doi.org/10.1021/acs.est.6b04308>
- Yanai, R. D., Yang, Y., Wild, A. D., Smith, K. T., & Driscoll, C. T. (2020). New approaches to understand mercury in trees: Radial and longitudinal patterns of mercury in tree rings and genetic control of mercury in maple sap. *Water, Air, & Soil Pollution*, 231(5), 231–248. <https://doi.org/10.1007/s11270-020-04601-2>
- Yang, Y., Yanai, R. D., Montesdeoca, M., & Driscoll, C. T. (2017). Measuring mercury in wood: Challenging but important. *International Journal of Environmental Analytical Chemistry*, 97(5), 456–467. <https://doi.org/10.1080/03067319.2017.1324852>
- Yu, Q., Luo, Y., Xu, G., Wu, Q., Wang, S., Hao, J., & Duan, L. (2020). Subtropical forests act as mercury sinks but as net sources of gaseous elemental mercury in South China. *Environmental Science & Technology*, 54(5), 2772–2779. <https://doi.org/10.1021/acs.est.9b06715>
- Yuan, W., Sommar, J., Lin, C.-J., Wang, X., Li, K., Liu, Y., Zhang, H., Lu, Z., Wu, C., & Feng, X. (2019a). Stable isotope evidence shows re-emission of elemental mercury vapor occurring after reductive loss from foliage. *Environmental Science & Technology*, 53(2), 651–660. <https://doi.org/10.1021/acs.est.8b04865>
- Yuan, W., Wang, X., Lin, C.-J., Sommar, J., Lu, Z., & Feng, X. (2019b). Process factors driving dynamic exchange of elemental mercury vapor over soil in broadleaf forest ecosystems. *Atmospheric Environment*, 219, 117047. <https://doi.org/10.1016/j.atmosenv.2019.117047>
- Yuan, W., Wang, X., Lin, C. J., Wu, C., Zhang, L., Wang, B., Sommar, J., Lu, Z., & Feng, X. (2020). Stable mercury isotope transition during postdepositional decomposition of biomass in a forest ecosystem over five centuries. *Environmental Science & Technology*, 54(14), 8739–8749. <https://doi.org/10.1021/acs.est.0c00950>
- Zayed, J., Loranger, S., & Kennedy, G. (1992). Variations of trace-element concentrations in red spruce tree rings. *Water, Air, & Soil Pollution*, 65(3–4), 281–291. <https://doi.org/10.1007/BF00479892>
- Zhao, Z., Wang, D. Y., Wang, Y., Mu, Z. J., & Zhu, J. S. (2015). Wet deposition flux and runoff output flux of mercury in a typical small agricultural watershed in Three Gorges Reservoir areas. *Environmental Science and Pollution Research International*, 22(7), 5538–5551. <https://doi.org/10.1007/s11356-014-3701-2>
- Zheng, W., Demers, J. D., Lu, X., Bergquist, B. A., Anbar, A. D., Blum, J. D., & Gu, B. (2019). Mercury stable isotope fractionation during abiotic dark oxidation in the presence of thiols and natural organic matter. *Environmental Science & Technology*, 53(4), 1853–1862. <https://doi.org/10.1021/acs.est.8b05047>
- Zheng, W., & Hintelmann, H. (2010). Nuclear field shift effect in isotope fractionation of mercury during abiotic reduction in the absence of light. *The Journal of Physical Chemistry. A*, 114(12), 4238–4245. <https://doi.org/10.1021/jp910353y>
- Zheng, W., Obrist, D., Weis, D., & Bergquist, B. A. (2016). Mercury isotope compositions across North American forests. *Global Biogeochemical Cycles*, 30(10), 1475–1492. <https://doi.org/10.1002/2015GB005323>
- Zhou, J., Obrist, D., Dastoor, A., Jiskra, M., & Ryjkov, A. (2021). Vegetation uptake of mercury and impacts on global cycling. *Nature Reviews Earth & Environment*, 2(4), 269–284. <https://doi.org/10.1038/s43017-021-00146-y>
- Zhu, W., Lin, C. J., Wang, X., Sommar, J., Fu, X., & Feng, X. (2016). Global observations and modeling of atmosphere–surface exchange of elemental mercury: A critical review. *Atmospheric Chemistry and Physics*, 16(7), 4451–4480. <https://doi.org/10.5194/acp-16-4451-2016>